



Sudan University of Science and Technology
College of Petroleum Engineering & Technology
Department of Exploration Engineering



Subsurface structural mapping Melut Basin using satellite gravity data

تخريط التراكييب تحت السطحيه لحوض ملوط باستخدام بيانات الاقمار

الاصطناعية للجاذبية

This dissertation is submitted as a partial requirement of B.Sc. degree (honor)
in Exploration Engineering

Prepared by :

- 1. Al-miqdad Hassan Hamed Alkdagry**
- 2. Abubaker Mohammed Ahmed Alshreef**
- 3. Khaled AbuBakr Mirghani**
- 4. Mohammed Abdolbasit abdorchman**

Supervisor :

Dr. Khalid AbdelRahman Elsayed Zeinelabdein

October 2015

الآية

بِسْمِ اللَّهِ الرَّحْمَنِ الرَّحِيمِ

قال تعالى:

﴿ولا يأتونك بمثل إلا جئناك بالحق وأحسن تفسيراً﴾

بِسْمِ اللَّهِ الرَّحْمَنِ الرَّحِيمِ

سورة الفرقان - (33)



Dedication

We dedicate this work to:

Our Fathers

*The one who taught us the
Meaning of principles and give.*

Our Mothers

*our power resource and the candle
that lighting our darkness*

Our brothers and our sisters

Our friends

The soft candle in our life

Our teachers

Our prideness icon

Acknowledgment

The favorness firstly and lastly for Allah who gave us the stenth and patience to do this work,

We would like to sent best wishes to supervisor,

Dr. Khalid AbdelRahman Elsayed Zeinelabdein

for his gaudiness and support to help us in generating perfect work, that by the will of Allah become a beneficial study.

We would like to thank our adorable friends, for helping us in many ways that no one could.

We would like to thank Dr. Eman abdAllah, Ustaza. Hanan Mohamed, Ustaz. Mohmmmed Salah, Ustaza. Amna Abdelmonem And Ustaza. Mai Alsadig for helping us.

Finally we would like to thank Ministry of Mineral.

May Allah bless them all.

ABSTRACT

Melut Basin is one of the largest and most important oil producing areas in South Sudan. It is located in the northeastern part of the South Sudan and is covered by a sedimentary succession of Cretaceous and Tertiary continental strata that attain a thickness of more than 5km in the depocentres of the basin.

Melut Basin is considered as one of the most perspective basins with respect to oil in South Sudan. Extensive exploration activities are going on in the northern part of this basin. Other parts are still unstudied and little is known about their prospectivity. The overall objective of the present study is investigate the subsurface structures of Melut Basin using the potential field data obtained from both ground measurement and satellite observations.

The method used in this study is Gravity method that depends on densities variations. For the present work various data types, from different sources (ground and satellite gravity data) were made available. That individually constitute part of the spatial information system pertaining to the Melut area have been used.

The difference between the ground and satellite gravity data is very minor. Accordingly, satellite gravity data used in present study. This is because satellite gravity data are better than the ground measurement.

Average method was used in order to separate the regional from the residual component of the gravity. The Derivatives of the Gravity were computed in order to study the presence of faults. Moreover, two profiles were constructed across the residual gravity map in an approximately SW-NE and NW-SE directions cutting the most prominent anomalies in the area. 2.5D Gravity modeling established to decipher the subsurface structure along two profiles in the study area.

The results of interpretation maps and profiles defined boundary of Basin, identified there was many Faults in the study area and computed depth of Basement along profiles.

الخلاصة

حوض ملوط من أكبر و اهم الاحواض الرسوبية المنتجة في دولة جنوب السودان ويقع في الجزء الشمالي الشرقي منها وقد تصل اعماقه الى اكثر من 5 كلم في مركز ترسيب الحوض.

تمت الدراسة في الجزء الشمالي لهذا الحوض بصورة جيدة ولكن مازال الجزء الجنوبي له فقير في كثير من المعلومات التي تصف الحوض بصورة جيدة . لذا كانت الدراسة الحالية هي وصف التراكيب التحت سطحية له باستخدام الطريقة الجاذبية التي تعتمد على الاختلاف في الكثافات بين الصخور في اجراء الدراسة الحالية. استخدمت بيانات الجاذبية المقاسة بواسطة جهاز القرافوميتر وايضا المقاسة بواسطة اقمار صناعية للدراسة الحالية.

وجد ان الاختلاف بين القراءات التي اخذت من الحقل والقراءات التي قيست بواسطة الاقمار الاصطناعية بسيط جدا بعد اجراء مقارنه بينهما ، لذا استخدمت قراءات الاقمار الاصطناعية للعمليات والتحليل للبيانات في الدراسة .

تم الفصل بين الجاذبية الاقليمية والمحلية وبعد ذلك حسب المشتقات للجاذبية وانشئت خرائط لكل منها. تم عمل قطاعين مختلفين على الشذوذ الموجوده في منطقة الدراسة باتجاهات جنوب غرب شمال شرق وشمال غرب جنوب شرق . وتم انشاء نمزجه في 2.5 اتجاه لهذه القطاعات .

من الدراسة الحالية تم التعرف على حدود الحوض ، عمق صخور الاساس والتراكيب الموجوده في الحوض وشكلها .

Table of Contents

الإيئة.....	I
Dedication	II
Acknowledgment	III
ABSTRACT	IV
الخلاصة.....	V
List of Figures:	VIII
List of Table	VIII
1. INTRODUCTION	1
1.1 Statement Of The Problem.....	1
1.2 Objectives Of The Study	1
1.3 Location Of The Study Area	1
1.4 Topography:	3
1.5 Climate and Vegetation.....	3
1.6 Drainage System	4
1.7 Population	6
1.8 Previous Studies On Petroleum Exploration	6
1.9 Methodology:	7
1.9.1 Materials :.....	7
1.9.2 Method:	7
1.9.3 Software:	7
2. REGIONAL GEOLOGY AND TECTONIC SETTING	8
2.1 Regional Geology.....	8
2.1.1 Basement Complex of The NUBA MOUNTAINS.....	9
2.1.2 Basement Complex Of The Ingessana Hills.....	10
2.1.3sedimentary Rocks Of Melut Basin And Vicinity.....	12
2.2 Tectonic Setting	15
2.3 Sudan Basins	16
.3 LITERATURE REVIEW	20
3.1 Geographic Information System (GIS)	20
3.2 Gravity Surveying	22
3.2.1 Introduction	22
3.2.2 Basic Theory	22
3.2.4 Earth's Gravitational Field And Its Relation To Exploration:	24

3.2.5 Gravity Measurements	25
3.2.6 Instruments For Measuring Gravity	26
3.2.7 Variation With Latitude	26
3.2.8 Variation With Elevation	27
3.2.9 Terrain Effect	27
3.2.10 Variation With Time	28
3.2.11 Variation With Geology	29
3.3 Satellite Gravity	29
4. DATA PROCESSING AND INTERPRETATION.....	30
4.1 Introduction	30
4.2 Ground Gravity	30
4.3 Satellite Gravity	30
4.5 Processing And Interpretation.....	34
4.5.1 Introduction	34
4.5.2 Bouguer Anomaly (Ba)	34
4.5.3 Regional-Residual Anomaly Separation	36
4.5.4 Derivatives Of The Gravity Field:.....	39
4.6 2.5D Gravity Modeling	44
5. CONCLUSION AND RECOMMENDATIONS.....	48
5.1 Conclusion:	48
5.2 Recommendations:	48
References.....	49

List of Figures:

Fig 1.1 : Location of study area.....	2
Fig 1.2 : Average temperaturesin Melut area.	4
Fig 1.3 : Rainfall in mm in Melut area.	4
Fig 1.4 : show the drainage system of the study area.....	5
Fig 2.1 : Geological map of the study area and vicinity (modified after GRAS, 2005).....	11
Fig 2.2 : Generalized geological map showing the main lithological units of Sudan and adjacent territories (modified after Vail, 1988).	14
Fig 2.3 : Structural map showing the major rift basins of Sudan and adjacent countries (modified after Pudloet al., 1997).	17
Fig 3.1 : Diagram illustrates the calculation of the gravity potential.	24
Fig 3.2 : Free Air, Bouguer and Terrain Effects.	28
Fig 4.1 : Showing comparison between satellite and ground gravity.....	33
Fig 4.2 : Showing Bouguer Anomaly Gravity map for Melut region. Contour interval is 5mGal. Crosses lines are gravity model profiles.	35
Fig 4.3 : The residual gravity map for study area. Contour interval is 5mGal.Black lines are the location of profiles used in gravity modeling.....	38
Fig 4.4 : First vertical derivative map and of the study area, on which the zero contours lines separates the positive from the negative anomalies.....	40
Fig 4.5 : The second vertical derivative map and of the study area, on which the zero contours line separates the positive from the negative anomalies.	41
Fig 4.6 : First horizontal derivative map for Melut region, with zero contours line.	43
Fig 4.7 : Geological model of profile (1).	45
Fig 4.8 : Second vertical derivative (SVD) along profile 1. F stands for Fault.....	45
Fig 4.9 : Geological model of profile (2).	46
Fig 4.10 : Second vertical derivative (SVD) along profile 2. F stands for Fault.....	47

List of Table

Table 4.1 : Sample of Ground data.	31
Table 4.2 : Sample of Satellite data and corrections.	32

1. INTRODUCTION

1.1 Statement Of The Problem

Melut Basin is considered as one of the most perspective basins with respect to oil in South Sudan. Extensive exploration activities are going on in the northern part of this basin. Other parts are still unstudied and little is known about their prospectively. Mapping of prospective zones for oil exploration in this area using potential field data will pave the road for future investigation efforts and narrow the search area, which in turn reduces both the cost of these activities and the required time.

1.2 Objectives Of The Study

The overall objective of the present study is investigate the subsurface structures of Melut Basin using the potential field data obtained from both ground measurement and satellite observations. This objective can be achieved fulfilling a number of specific objectives including:

- Checking the reliability of satellite gravity data through the comparison with ground measurement.
- Processing and interpretation of satellite gravity data.
- Delineation of structural faults that govern the geometry of the basin.
- Modeling the subsurface geological structure.

1.3 Location Of The Study Area

Melut Basin is one of the largest and most important oil producing areas in South Sudan. It is located in the northeastern part of the South Sudan and is covered by a sedimentary succession of Cretaceous and Tertiary continental strata that attain a thickness of more than 5km in the depocentres of the basin.

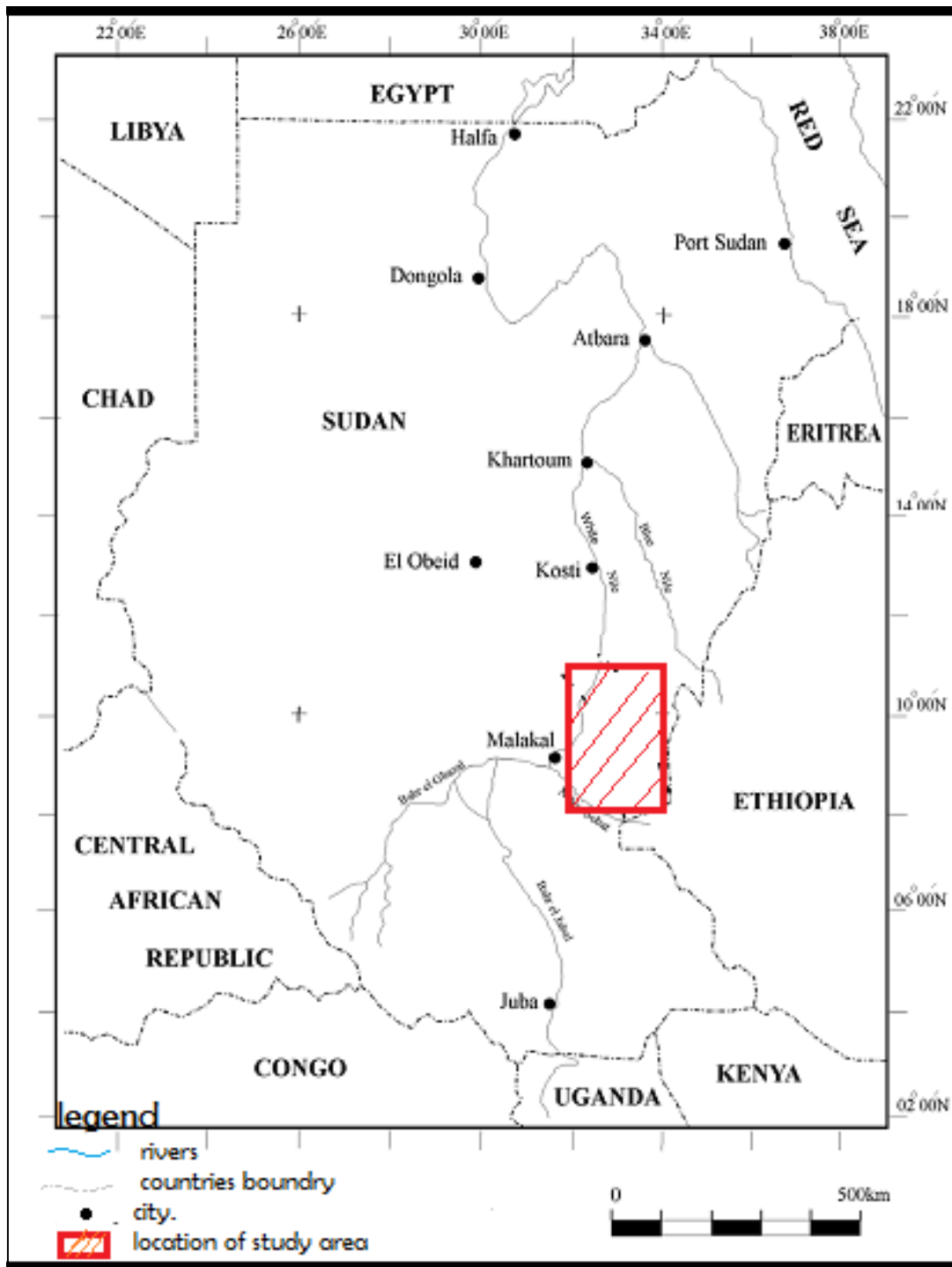


Fig 1.1 : Location of study area.

Melut Basin is part of the Central African Rift System it trends in the NW-SE direction and terminates against the Central African Shear Zone (CASZ) Fig (1.1). It trends generally NNW direction , approximately bounded by the longitudes 32° 00'E and 34° 00' E and latitudes 8° 00'N and 10° 30' N. The basin lies about 670 km south of Khartoum; extending about 400 km in a NNW direction from the Ethiopian border into South Sudan the maximum width of the basin about some 200 km Fig(1.1). The terrain in this area is flat.

1.4 Topography:

The area is characterized by flat, low lying and vast plains, with black cotton soils. The study area occupies a topographically low land adjacent to the two uplifted basement blocks of the Ingessana Hills in the northeast and the Nuba Mountains in the northwest. Apart from some isolated sandstone outcrops, the Melut Basin and the surrounding areas are essentially flat land covered by superficial deposits of Quaternary age. The area has a mean ground elevation of about 395 m above sea level, and the difference between the highest and the lowest places is less than 15 m.

1.5 Climate and Vegetation

Melut is highly difficult, if not impossible, to forecast what the weather will be like at a certain time in a very precise place. The climate is generally hot and the area is swampy in the rainy season, between June and October, and increasingly dry during the rest of the year (Fig. 1.2 and 1.3).Savannah grasslands and acacia trees are the typical vegetative cover.

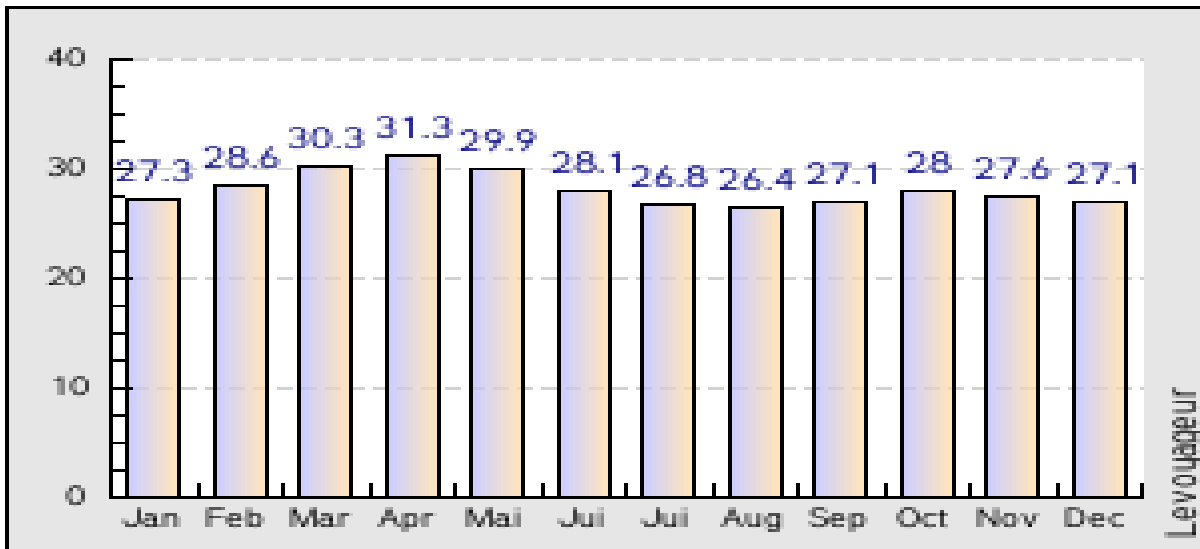


Fig 1.2 : Average temperatures in Melut area.

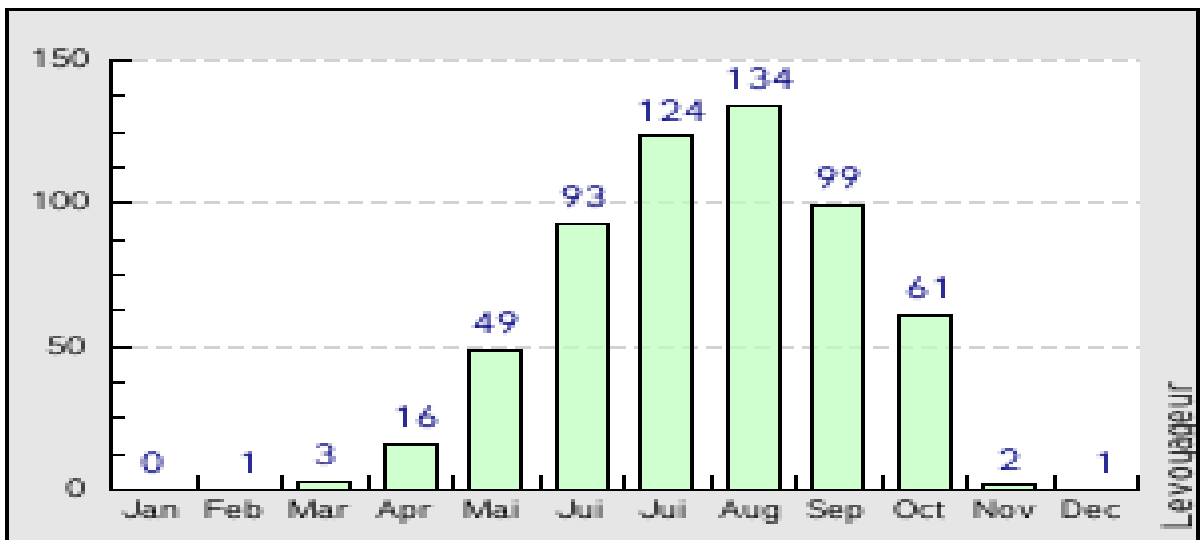


Fig 1.3 : Rainfall in mm in Melut area.

1.6 Drainage System

The drainage system generally runs towards the northwest, of which the White Nile and its tributaries represent the main drainage elements. Melut County is part of a flat clay plain with seasonal streams (called Khor) running from the east to the White Nile in the west. The banks of Nile and its small seasonal tributaries such as river *Awilwil* and *Thor Ager* criss-crossing the county determine the settlement patterns of the villages. These rivers are the main sources of drinking water, fishing grounds and watering points for the community livestock especially

during the dry season Fig(1.4). River Nile is also central to long distance migration and transport into and out of Melut and the adjoining counties.

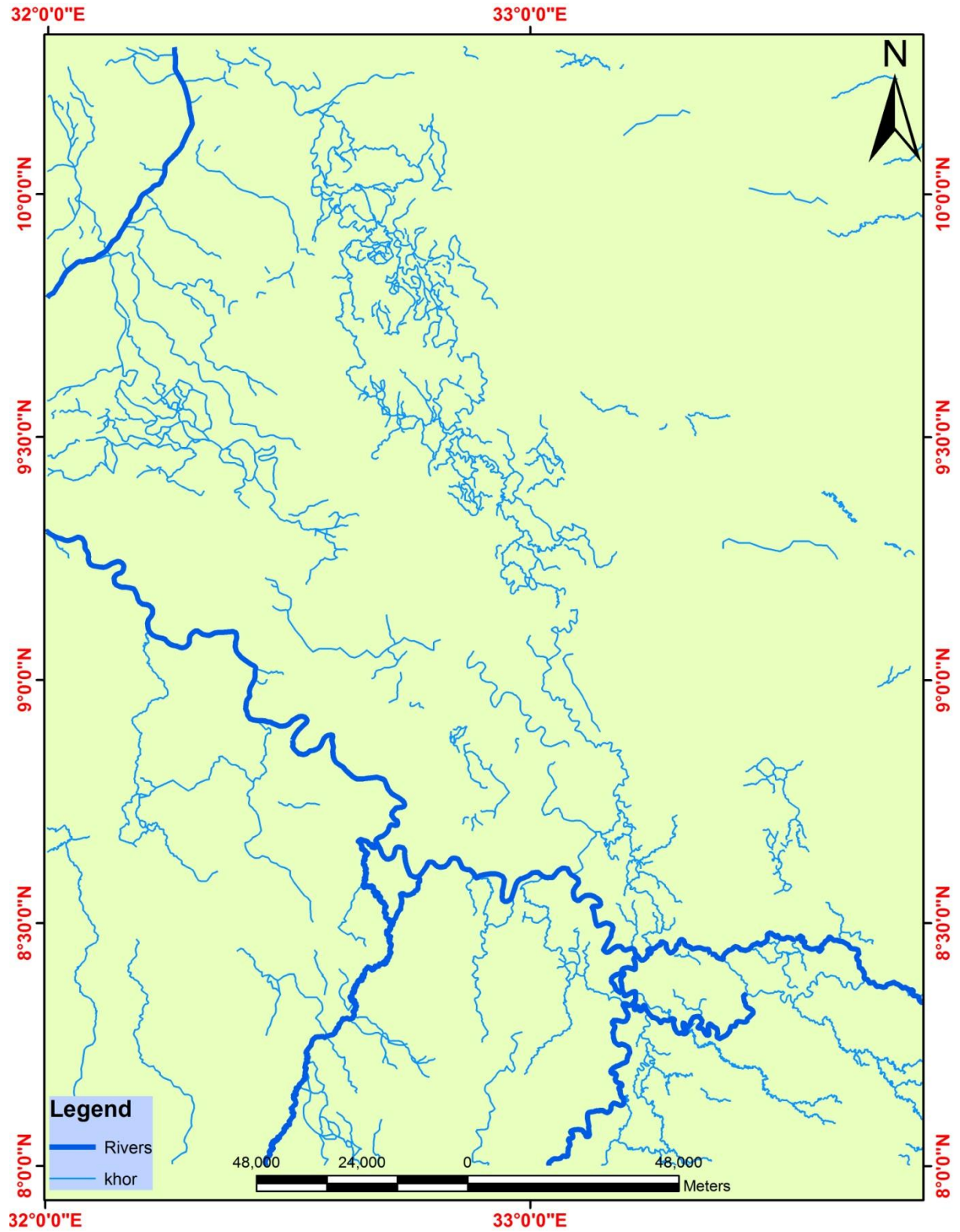


Fig 1.4 : show the drainage system of the study area.

1.7 Population

There are different communities coexisting in Melut County. The major ones being Dinka, Shilluk, Burun, Furs, Nubians and Nuer. Other communities are in minority (Murle and Anyuak). The population is estimated at 128, 571 persons.

The predominant livelihoods of the communities in this region are agro-pastoralism, formal and informal employment and small scale trading. Fishing is practiced on a small scale. An important proportion of the population relies heavily on kinship support.

Melut County is located along the migratory path of the Nile River and road network. Therefore it counts many migrants that are mainly settling in the cosmopolitan areas of Melut, Paloch and Galdora areas.

1.8 Previous Studies On Petroleum Exploration

Exploration for oil in the Melut Basin was first attempted by Chevron Overseas Petroleum Inc. in 1975. Magnetic and gravity surveys followed by seismic investigations were carried out in an area covering almost completely the southern part of Sudan. Acquiring good results from the geophysical surveying, Chevron was encouraged to drill five exploratory wells in the Melut Basin from June 1981 to May 1982 in which oil was discovered in some of these wells. Shortly after that, Chevron relinquished the area after the evaluation of the Adar/ Yale oil field. The activity halted in the area until August 1995, when Gulf Petroleum Company Sudan (GPCS) signed a production-sharing contract with three companies and started production in Adar-Yale oil field. This agreement was replaced in October 2001 by a consortium named Petrodar (PDOC). According to information found at <http://www.petrodar.com/partners.html>, the shareholder of PDOC is a consortium of five international exploration and production oil companies: The China National Petroleum Corporation (CNPC) 41%, Petroliam Nasional Berhard (PETRONAS) 40%, Sudan Petroleum Company Ltd. (SUDAPET) 8%, China Petroleum and Chemical Corporation (SINOPEC) 6% and 5% for Al Thani Corporation.

Extensive exploration and development activities carried out by PDOC in the study area have resulted in important discoveries of new oil fields and increased production volumes (personal communication with PDOC staff).

1.9 Methodology:

1.9.1 Materials :

In order to fulfill the objectives of the present study, different data types have been utilized, these include:

- Landsat 7 ETM image, path (171-173) and row (53 and 54), in Digital format, including seven spectral bands, acquired on 2000.
- Ground gravity, which represents about 1251 points, has read using gravimeter device and within the limits of the study area .in the form bouguer anomaly (BA).
- . Satellite gravity grid data obtained from the Satellite Geodesy located at latitude (8N, 9N and 10N.) and longitude (20° 00'E to 38° 00'E), include the study area between these lines in the form of free air anomaly (FAA).
- The data obtained from open file of the Ministry Of Mineral and Energy.

1.9.2 Method:

The gravity data was originally provided as Bouguer Anomaly(BA) were the satellite gravity was originally as free air anomaly (FAA) delivered together with the elevation data for each point. This combination of data was used to compute Bouguer Anomaly (BA) for the study area .after that import to GIS and draw map to BA and contour ,this map used to separation between regional and residual gravity, Furthermore, different derivatives (first vertical derivative, second vertical derivative and first horizontal derivative). We are used the residual map to draw two profiles passes Crosse the largest number of the faults in the area. This profiles are imports to the graph model to export profiles figure. Explain the fault zone were computed from the Bouguer anomaly values. The Bouguer anomaly and the derived values were interpreted in terms of variations in litho logical units, which were constrained by the surface exposures where available. BA data, derivatives and residual were all imported into the GIS environment, where data integration and analysis was carried out to facilitate the production of the final geological map of the study area.

1.9.3 Software:

Some software using in this study:

- **ArcGIS program** was used to generate maps used in the interpretation of subsurface structures.
- **Geosoft OasisMontag** was used to compute Derivatives for the Bouguer anomaly gravity data.
- **Gravmodel program** was used to generate modeling for two profiles.

2. REGIONAL GEOLOGY AND TECTONIC SETTING

2.1 Regional Geology

Whiteman (1971) and Vail (1978) shortly described the geology of the study area and the adjacent Territories in the general context of the geology of the Sudan. Being a target for hydrocarbon Exploration, the study area became a focus for detailed geological investigations during the past three Decades. Prior to chevron's exploration program in Sudan from 1975 to 1985, it was generally believed that the geology of the central Sudan was characterized by shallow basins filled by thin Sedimentary cover, unconformably overlying the Precambrian basement rocks.

This concept was later modified by the results of the geophysical work conducted by chevron, which showed the presence of deep rift structures filled by thick non-marine Mesozoic and Cenozoic sequences related to the Central African Shear Zone (CASZ, Schull, 1988). Based on geophysical investigations (RRI and GRS, 1991), geological interpretation (Schull, 1988) and palynological information obtained from boreholes (Kaska, 1989; Eisawi, 2007), the stratigraphic Column of the study area can be summarized as follows:

- Quaternary cover
- Unconformity
- Tertiary strata
- Unconformity
- Late Cretaceous strata
- Unconformity
- Precambrian Basement Complex

The Melut Basin is characterized by flat plains, composed of older alluvium, sand plains, wadi deposits, lacustrine deposits and alluvial fans Fig. (2.1), This plain area is surrounded by regionally metamorphosed Precambrian and Paleozoic rocks and minor (syn-late- to post-tectonic) Mesozoic/Cenozoic intrusive and extrusive igneous rocks. These rocks are exposed

northeast and northwest of the study area in the Ingessana Hills and Nuba Mountains, respectively Fig. (2.3). The surrounding basement terrains represent the source area for the sediments filling the Melut Basin (Schull, 1988). A brief account on the geology of the two massifs will be given in the following section:

2.1.1 Basement Complex of The NUBA MOUNTAINS

The Precambrian Basement Complex of the NE Nuba Mountains is made of high-grade gneisses and a low-grade greenschist volcano-sedimentary sequence. The tectonic contact between the two groups is marked by the Kabusophiolitic mélange zone (Abdelsalam and Dawoud, 1991). Based on previous investigations (Whiteman, 1971; Vail, 1978; El Ageed and El Rabaa, 1981; HirdsandBrinkmann, 1985; Abdelsalam and Dawoud, 1991), the stratigraphic and tectonic subdivisions of the Basement Complex of the NE Nuba Mountains can be summarized as follows:

- Post-orogenic granites
- Syn-late orogenic granites
- Kabus ophiolitic mélange rock assemblage
- Low-grade volcano-sedimentary sequence
- High-grade gneisses

The gneisses are exposed as low-lying bouldery outcrops, overlain in places by a thin sedimentary cover of Quaternary age. They comprise mainly quartzo-feldspathic gneisses commonly associated with small lenses of concordant amphibolites and local migmatites (Vail, 1978). The second unit of the basement rocks comprises the low-grade greenschist-facies assemblage (metavolcanic and metasediments) that includes marble, mica schist, quartzites, graphite and chlorite schists Fig. (2.1). They occur as low isolated outcrops and outstanding ridges generally delineating the configuration of the fold structures and forming intercalated bands of met sedimentary and metavolcanic rocks that probably represent different depositional and volcanic eruption phases (Abdelsalam and Dawoud, 1991). The ophiolite zone marks the suture between the low-grade greenschist-facies assemblage (island arc terrain) and the high-grade gneisses of continental origin in the northeastern Nuba Mountains Fig. (2.1). The rocks of this unit occur as discontinuous lenticular bodies in an imbricate structure (Abdelsalam and Dawoud, 1991).

The older metamorphosed basement rocks were intruded by syn-late orogenic granites, which predate the younger post-orogenic igneous complexes of the Sudan (El Ageed and El Rabaa, 1981).

The youngest unit of the basement complex is the post-orogenic granite reported from the northern Nuba Mountains at Jebel Ed Dair and Jebel Dumbeir. These are non-foliated, shallow-level granitic bodies and volcanics that occur as ring complexes and discrete bodies, intruded during the Paleozoic around 542 Ma (Vail, 1988). They are composed mainly of alkali syenites, alkali granites, and gabbros Fig.(2.2).

2.1.2 Basement Complex Of The Ingessana Hills

The Basement Complex of the Ingessana area consists of quartzo-feldspathic gneisses in which bands of marble, mica-schist and quartzite are developed in places. Varieties of igneous rocks were intruded into the metamorphosed basement. The largest units of the basement rocks are foliated granites and granodiorites, which may be syn-late tectonic intrusions. They are in contrast to smaller cross-cutting unfoliated post-orogenic granite plutons (Vail, 1978).

The most striking intrusive bodies are the numerous ultra basic and basic rocks; the most significant is that of the Ingessana Hills Fig. (2.1). This body is about 25 km in diameter and consists of serpentinitised unit, talc- carbonate- schists, peridotite, epidiorite, norite and gabbro. Lenses of chromite are present, especially in the southwest. The mafic rocks are intruded by a circular plug of acid rocks, namely the Bau granite (Vail, 1978).

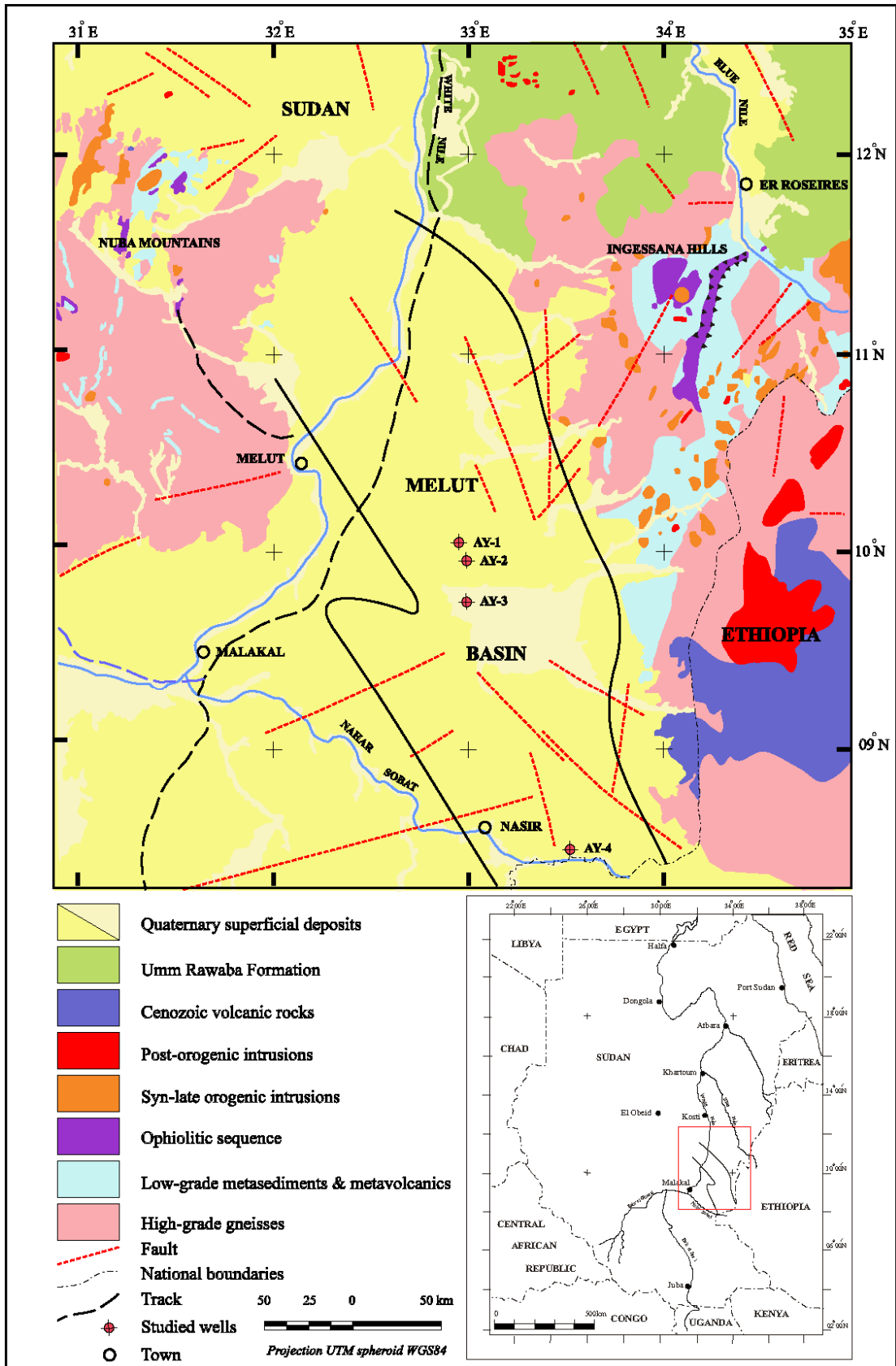


Fig 2.1 : Geological map of the study area and vicinity (modified after GRAS, 2005).

2.1.3 sedimentary Rocks Of Melut Basin And Vicinity

A brief account of the main sedimentary units in the study area and its vicinity will be given in this section.

2.1.3.1 Paleozoic Sediments

Rocks of Paleozoic age were only reported from far northwestern and northeastern Sudan (Klitzsch, 1984; Klitzsch and Lejal-Nicol, 1984). Trace fossils, mainly *Cruziana acacensis*, *Skolithos* sp., *Harlania harlani* and others were reported from these sediments. The recorded trace fossils were interpreted to indicate marginal marine palaeoenvironment with rare fluvial input. Paleozoic sediments were also reported, near the Melut Basin, from west-central Ethiopia (Kazmin, 1973). They are overlain by the Late Triassic to Early Jurassic (?) Adigrat Sandstone Formation Fig. (2.2).

Awad (1994) reported the presence of reworked scolecodonts of probable marine origin associated with Late Jurassic to Barremian pollen and spores in the Khartoum Basin. He concluded that such forms indicate possible occurrence of Paleozoic marine rocks near the Khartoum Basin that had been partially or completely eroded and transported into the basin during the Tithonian and Barremian.

2.1.3.2 Mesozoic Sediments

Within the sequence of the Melut Basin, Mesozoic strata are only known from the subsurface. The nearest outcropping Mesozoic unit, termed the Adigrat Sandstone Formation, is reported in Ethiopia (Getaneh, 1981) along the Blue Nile gorge, approximately 250 km east of the study area Fig. (2.2).

Based on the association of pollen and spores, Hankel proposed a Late Triassic to Early Jurassic age for this unit in the Ogaden Basin.

2.1.3.3 Cenozoic Sediments

Cenozoic sediments in the Melut Basin and its surroundings are represented by Paleogene/ Neogene strata (identified from the subsurface of the basin), the Umm Ruwaba Formation and the surface deposits Fig.(2.1).

The term Umm Ruwaba Formation refers to the unconsolidated fluvial deposits of the White Nile drainage system in central and southeastern Sudan (Andrew, 1948). The unit consists of unconsolidated sands, clayey sands and clays with some gravel beds and generally exhibits rapid facies variation Fig. (2.1). The sandy material (beside quartz) contains considerable amounts of feldspar, kaolin and sodic plagioclase (El Shaafie, 1975). At the type locality (Umm Ruwaba town), the unit is 278.6 m thick but may attain a thickness of 335 m or more in the eastern Kordofan (Vail, 1988).

The youngest unit in the sequence of the Melut Basin is represented by the superficial deposits of Quaternary age Fig. (2.1).

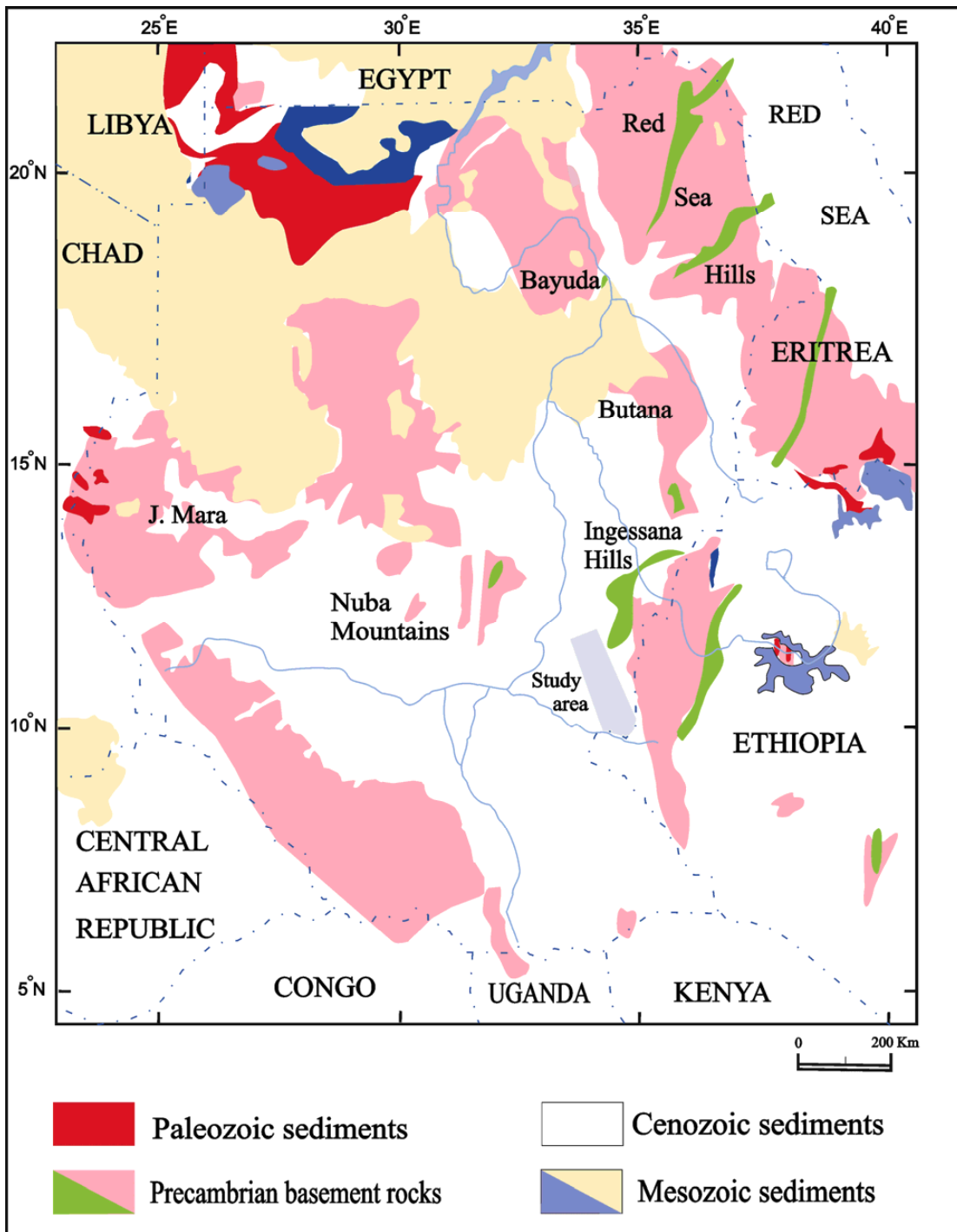


Fig 2.2 : Generalized geological map showing the main lithological units of Sudan and adjacent territories (modified after Vail, 1988).

2.2 Tectonic Setting

The major structural features of the Melut Basin and the surrounding areas are reviewed in this section and illustrated in Fig(2.3). A detailed, illustrated account on the subsurface structure of the southern Sudanese basins can be found in Schull (1988).

In terms of their evolution, Sudan's interior basins have been related to the west and central African rift system (CASZ; Schull,1988), formed in the Late Jurassic to Early Cretaceous. The shear stress resulting from the separation of Africa and South America and the subsequent opening of the South Atlantic Basin has been transferred along the Central African Fault Zone. The structural development of the Muglad Basin is marked by three major rift cycles followed by subsidence characterized by coarsening upward sequences of clastic sediments. The Muglad, Melut and Blue Nile are the three major sedimentary basins in the area and all three are likely to have been affected by similar tectonic events (Schull,1988). These rift events consist of:

- Early rifting, which occurred in the late Jurassic to early Cretaceous (130-150 Ma). It was the strongest phase of rifting and lasted until near and Albian .
- Intermediate rifting, which took place in the Senonian to Turonian and resulted in the development of rift lakes and deposition of lacustrine and floodplain sediment of the Aradiba Formation with associated minor volcanics.
- A late rifting event in the late Eocene to Oligocene probably related to the opening of the Red Sea and East African Rift.
- A subsequent sag phase in the Middle Miocene has resulted in gentle subsidence with little faulting.

The age estimates are poorly constrained due to the sparse palynological data. The recognition of the three rift cycles is based on the identification of three regionally correlative depositional cycles, which are particularly evident in the Muglad Basin. Each cycle boundary is locally expressed by subtle angular unconformity.

These movements led to the creation of a complex system of linked extensional and transtensional sub-basins. The sub-basins typically have a half-graben geometry that was modified by subsiding reactivation during younger rift cycle. These graben structures generally trend NW-SE and are arranged in an en-echelon pattern.

2.3 Sudan Basins

Five NW-SE oriented continental rifts are now known to cross Sudan and South Sudan, defining an extensional province 1000 km wide and with length of at least 800 km parallel to the strike from north to the south. These rifts are Atbara, Blue Nile, White Nile (Melut basin), Abu Gabra-Muglad and Bahr El Arab rift are referred to collectively as the south Sudan rift in common, such as at Kosti, Umm Ruwaba basins of the White Nile rift and Sag El Naam basin. Generalized geological map is presented in shows the main lithological units of Sudan and adjacent territories which was modified after Vail (1988).

The Bahr El Arab rift comprises two major structures, the Baggara graben and Sudd graben. The Baggara graben covers the area between the Nuba Mountains in the east and the Central African Republic in the west. In the north it is defined by the faulted Mesozoic deposits south of Darfur dome. North of this line the Mesozoic deposits crop out in the form of chain of low lying flat topped hills covered by lateritic deposits, and extend for a distance of more than 200 km. South of the faulted zone the Mesozoic sediments are found below the surface and are known from the borehole records and remnants of sandstone and laterites cropping out along Bahr El Arab.

The Sudan graben is bounded in the Nuba Mountains and the Adok ridge in the northeast, in the west and southwest by uplifted basement ridge which marks the Nile-Congo divide, and in east basic volcanic extensions of the East African rift. The basin within Babanusa trough is defined by the extensive faulting system extending in NW-NE and E-W. The graben and horst indicate a step-like subsidence of separate blocks. The intensity of the faulting and the subsidence increase southward, most of these Basin are asymmetrical half graben and characterized by small extension feature, generally less than 10% to maximum of about 30% (Jorgensen and Bosworth 1989, Mann, 1989).

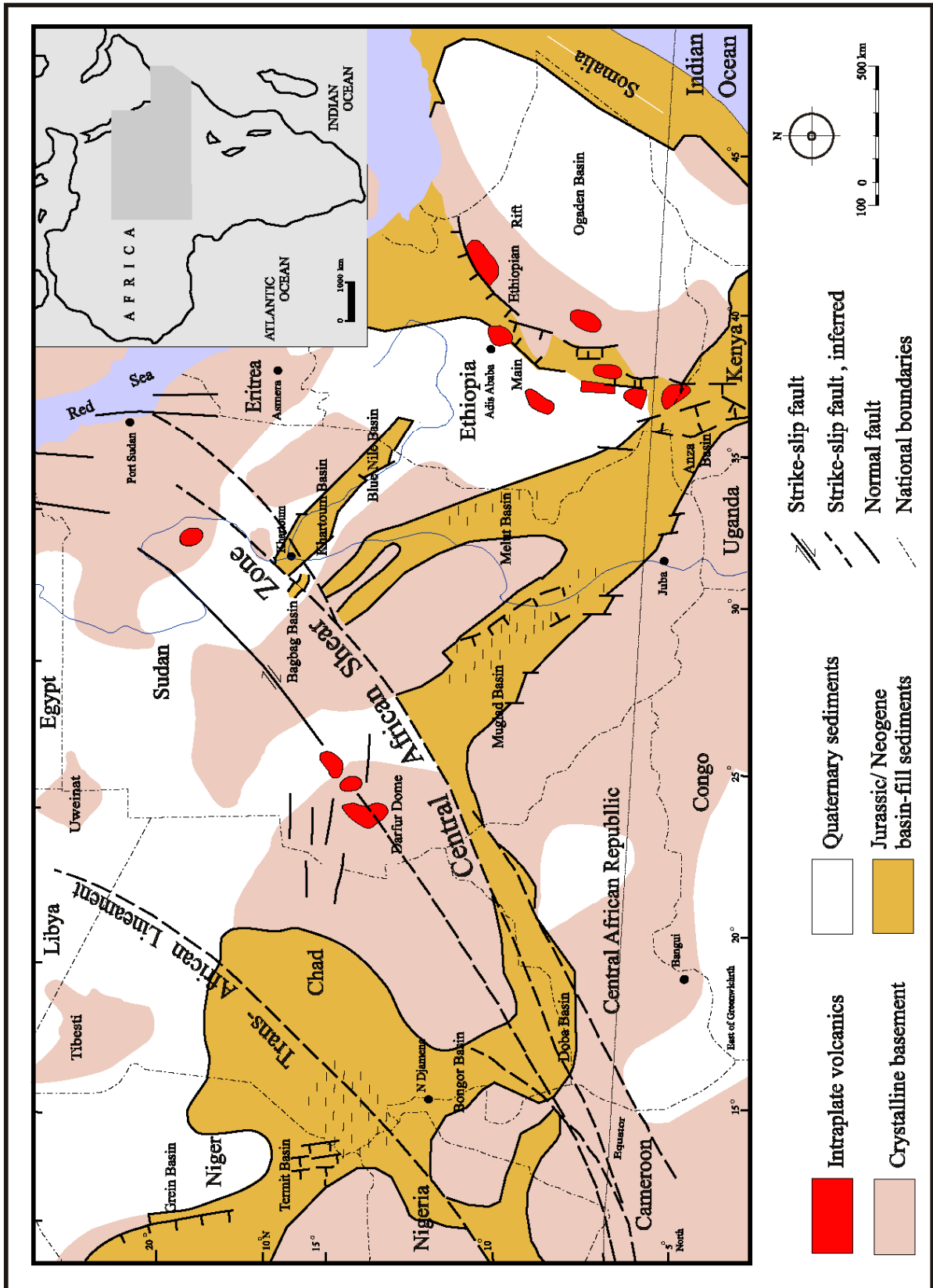


Fig 2.3 : Structural map showing the major rift basins of Sudan and adjacent countries (modified after Pudloet al., 1997).

Generally, along the strike the half graben is arranged in an en-chelon or staggered fashion, connected by accommodation zone. The direction of dominant stratal dip, commonly reverses across accommodation zones. This result in the accommodation zones displaying symmetric graben perpendicular to the rift axis (Coffield and Smale, 1987; Coffield and Schamel 1989). Figure (2.3) is detailed geological map shows the main lithological unit in the study area.

The stratigraphic successions of these basins are:

1. In Umm Ruwaba basin, the age of the older section is not known. It is overlain with angular unconformity by gently dipping sequence of Late Cretaceous to Paleocene sandstones, siltstones and shale.
2. In Blue Nile, the lower section will be tentatively assigned to the Late Jurassic or Early Cretaceous. The uppermost, un-faulted sequence is Miocene-Recent and is post-rifting in origin.
3. The While Nile Rift is shifted in a left-stepping fashion between Umm Ruwaba and Daragil. The offset comprises an accommodation zone which is an example of strata in Daragil are dated by Micropaleontology to Eocene-Oligocene and possibly Early Miocene; with Miocene-Recent post (Schull, 1988).
4. Khartoum Basin is probably the most structurally complex basin in the Sudan. This not only because it was reactivated in the Late Cretaceous, but also because it underwent significant inversion. Seismic stratigraphic relationships indicate that inversion occurred during deposition of the lower part of the Tertiary section and resulted in east-west shortening. The Khartoum basin bounding fault now resembles the Sunda Folds documented in the inverted basin of Indonesia (Bosworth, 1992).
5. Melut Basin: stratigraphically the area composed of sand shale intercalations of continental origin varying in sand and organic content upon the environment of deposition. The reservoir rocks were originally derived from the Precambrian and Cambrian gneissic basement. The multiple phases of rifting lead to episodic variations in basin subsidence that influence the stratigraphic evolution of the study area. Eleven (11) Lithostratigraphic units have been established in the Melut basin: Al-Gager Formation, al-Rank Formation, Galhak Formation, Melut Formation, Samma Formation, Yabus Formation, Adar Formation, Jimidi Formation,

Miadol Formation, Daga Formation and Agor Formation in ascending order. No rocks of Paleozoic to Jurassic age have been recognized in the drilled wells in the study area. Melut Basin is covered by superficial deposit of the Quaternary age as black cotton soil (Eisawi, 2007). Alluvial stream, wadi sediments and swamp deposits controlled by the main accommodation zone in the basin.

3. LITERATURE REVIEW

3.1 Geographic Information System (GIS)

GIS are computer-based systems that enable users to collect, store, process, analyze and present spatial data. It provides an electronic representation of information, called spatial data, about the Earth's natural and man-made features. A GIS references these real-world spatial data elements to a coordinate system. These features can be separated into different **layers**. A GIS system stores each category of information in a separate "layer" for ease of maintenance, analysis, and visualization. For example, layers can represent terrain characteristics, census data, demographics information, environmental and ecological data, roads, land use, river drainage and flood plains, and rare wildlife habitats. Different applications create and use different layers.

A GIS can also store attribute data, which is descriptive information of the map features. This attribute information is placed in a database separate from the graphics data but is linked to them. A GIS allows the examination of both spatial and attribute data at the same time. Also, a GIS lets users search the attribute data and relate it to the spatial data. Therefore, a GIS can combine geographic and other types of data to generate maps and reports, enabling users to collect, manage, and interpret location-based information in a planned and systematic way. *In short, a GIS can be defined as a computer system capable of assembling, storing, manipulating, and displaying geographically referenced information.*

GIS systems are dynamic and permit rapid updating, analysis, and display. They use data from many diverse sources such as satellite imagery, aerial photos, maps, ground surveys, and global positioning systems (GPS).

The GIS process consists of the following steps(Sabins, 2000):

- Compile source data and prepare the various original geographic data sets, which may consist of multi-spectral images (Landsat, AVHRR), contour maps, thematic maps

(climate, soils, others). At this stage the different data sets are in raster format and cover the same area.

- Geocode source data: This is the process of resampling each data set to a uniform pixel size that is registered to a geographic coordinate system.
- Derive attributes: A data set that is suitable for analysis is called attribute such as land cover maps and each spectral band of multi-spectral image is an attribute. The collection of geocoded attribute data is often called input data.
- Analyze attribute data: the attribute data are digitally processed to produce the desired information.
- Display results: the final display of a GIS session is typically a map with the desired information shown in colors or patterns.

Geographic features can be categorized into two types: the discrete and the continuous data. The discrete data are the distinct features that have a location and shape and constitute spatially well-defined features (e.g. rivers, lineaments, dykes and house). The discrete data are generally represented in the vector format. Continuous data are borderless and non-distinctive values that change gradually (e.g. pollution zone, temperature and rainfall zonation).

3.2 Gravity Surveying

3.2.1 Introduction

In gravity surveying, the subsurface geology is investigated in the basis of variation in the Earth's gravitational field generated by difference of density between subsurface rocks. The gravity method is a method of geophysical exploration, which is used to give information about the density distribution in the subsurface where simple and reasonable density contrasts exist. The method is generally applicable in reconnaissance surveys for basinal structures and regional mapping. It is equally important in controlling small-scale features such as fracture zones and mineral concentrations. The physical property is density; an underlying concept is the idea of a *causative body*, which is a rock unit of different density from its surroundings.

A causative body represents a subsurface zone of anomalous mass and causes a localized perturbation in the gravitational field known as a gravity anomaly. A very wide range of geological situations give rise to zones of anomalous mass that produces significant gravity anomalies.

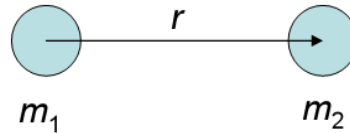
On a small scale, buried relief on a bedrock surface, such as a buried valley, can give rise to measurable anomalies. On a larger scale, small negative anomalies are associated with salt domes. On a larger scale still, major gravity anomalies are generated by granite plutons or sedimentary basins. Interpretation of gravity anomalies allows an assessment to be made of the probable depth and shape of the causative body.

The ability to carry out gravity surveys in marine areas or, to a lesser extent, from the air and space extends the scope of the method so that the technique may be employed in most areas of the world.

3.2.2 Basic Theory

The basis of the gravity survey method is Newton's Law of Gravitation, which states that the force of attraction F between two masses m_1 and m_2 , whose dimensions are small with respect to the distance r between them, is given by:

$$F = \frac{Gm_1m_2}{r^2}$$



where: G is the Gravitational Constant:

$$G = 6.67 \times 10^{-11} (SI) (Nm^2 Kg^{-2})$$

Consider the gravitational attraction of a spherical, non-rotating, homogeneous Earth of mass M and radius R on a small mass m on its surface. It is relatively simple to show that the mass of a sphere acts as though it were concentrated at the centre of the sphere and by substitution in equation:

$$F = \frac{GM}{R^2} m = mg$$

Force is related to mass by an acceleration and the term $g = GM/R^2$ is known as the gravitational acceleration or, simply, *gravity*. The weight of the mass is given by mg .

3.2.3 GRAVITATIONAL POTENTIAL

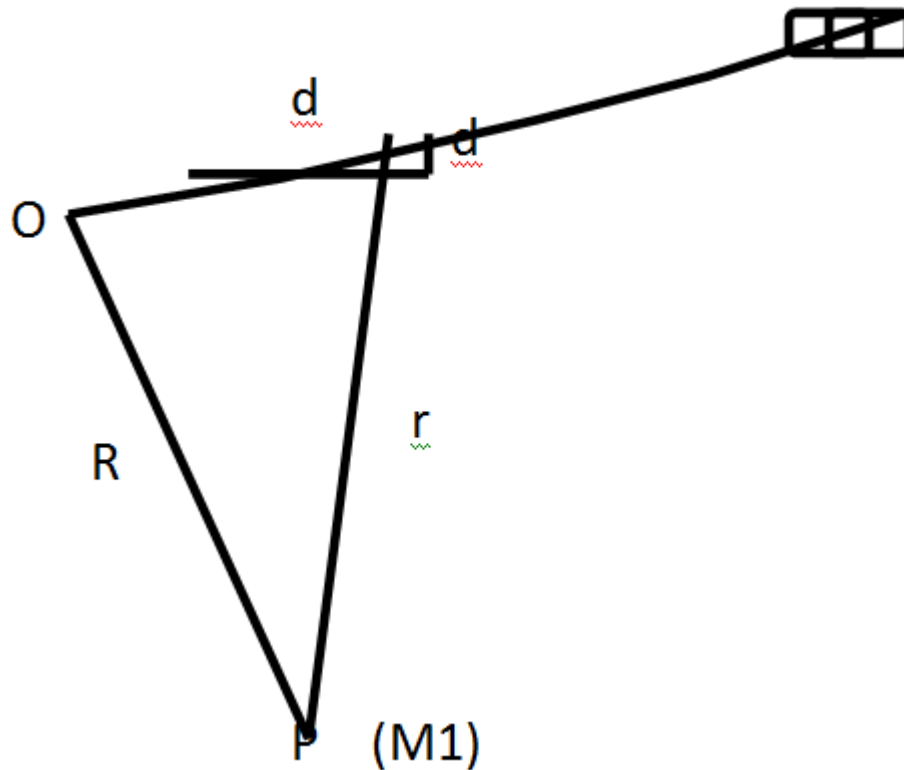
The potential at any point in gravitational field is defined as the work required for gravity to move a unit mass from an arbitrary reference point “usually at an infinite distance” to the point.

If the force per unit mass equals acceleration at distance $(r) = Gm_1/r^2$, the work to move the unit mass through the distance ds in the direction of P (Fig. 3.1)

$$\text{the work} = Gm_1 dr / r^2$$

The work U done to move the unit mass from infinity to O in the field of m_1

$$U = Gm_1 \int_{\infty}^R \frac{dr}{r^2} \qquad U = Gm_1 \frac{1}{r} = \frac{Gm_1}{R}$$



■ **Fig 3.1 : Diagram illustrates the calculation of the gravity potential.**

Whereas the gravitational acceleration g is a vector quantity, having magnitude and direction (vertically downwards), the gravitational potential U is a scalar, having magnitude only. The first derivative of U in any direction gives the component of gravity in that direction.

Consequently, a potential field approach provides computational flexibility. Equipotential surfaces can be defined on which U is constant. The sea-level surface, or *geoid*, is the most easily recognized equipotential surface, which is everywhere horizontal, that is, at right angles to the direction of gravity.

3.2.4 Earth's Gravitational Field And Its Relation To Exploration:

- If the earth is a perfect sphere and completely homogeneous in composition, then the gravity field at the surface would be identical all over the entire planet.

- The shape of the earth is practically spheroidal, bulging at the equator and flattened at the poles.
- The gravity measurements on the earth's surface depends on five factor:
 1. Latitude.
 2. Elevation.
 3. Topography and surrounding terrain.
 4. Earth tides.
 5. Variation in density of the subsurface.

3.2.5 Gravity Measurements

Since gravity is acceleration, its measurement should simply involve determinations of length and time. They are two type of gravity:

1. Absolute gravity
2. Relative gravity

However, such apparently simple measurements are not easily achievable at the precision and accuracy required in gravity surveying. The measurement of an absolute value of gravity is difficult and requires complex apparatus and a lengthy period of observation. Such measurement is classically made using large pendulums or falling body techniques (see e.g. Nettleton 1976, Whitcomb 1987), which can be made with a precision of 0.01 gu. Instruments for measuring absolute gravity in the field were originally bulky, expensive and slow to read (see e.g. Sakuma 1986).

The measurement of relative values of gravity, that is, the differences of gravity between locations, is simpler and is the standard procedure in gravity surveying. Absolute gravity values at survey stations may be obtained by reference to the International Gravity Standardization Network (IGSN) of 1971 (Morelli *et al.* 1971), a network of stations at which the absolute values of gravity have been determined by reference to sites of absolute gravity measurements. By using a relative reading instrument to determine the difference in gravity between an IGSN station and a field location the absolute value of gravity at that location can be determined.

Previous generations of relative reading instruments were based on small pendulums or the oscillation of torsion fibers and, although portable, took considerable time to read. Modern

instruments capable of rapid gravity measurements are known as *gravity meters* or *gravimeters*.

Gravimeters are basically spring balances carrying a constant mass. Variations in the weight of the mass caused by variations in gravity cause the length of the spring to vary and give a measure of the change in gravity. The extension of the spring is proportional to the extending force. The necessity for the spring to serve a dual function, namely to support the mass and to act as the measuring device, severely restricted the sensitivity of early gravimeters, known as stable or static gravimeters.

3.2.6 Instruments For Measuring Gravity

The instruments used are divided into two main types according to their way of measuring:

A) Instruments measure absolute gravity acceleration.

1- Falling body (weight).

2 -Pendulum

B) Instruments measure relative gravity acceleration:

1- Portable Pendulum.

2- Torsion balance.

3- Gravimeters (stable “static” and unstable).

Unstable Gravimeters are now widely used instruments and have several characters than other instruments (Worden, La Coste & Romberge gravimeters) are widely extensively used.

3.2.7 Variation With Latitude

The formula for the general increase of g with latitude θ , based on the most recently accepted spheroid approximation, is given by:

$$g = 978031.8 (1 + 0.0053024 \sin^2 \theta - 0.0000058 \sin^2 2\theta)$$

Where: g is the predicted value of gravity at latitude θ and 978031.8 is the value of gravity at the equator. The equation with the above constants is also known as the International Gravity Formula 1967. This equation includes both the Newtonian attraction of the Earth as a spheroid and the centrifugal force caused by its rotation about its axis.

3.2.8 Variation With Elevation

3.2.8.1 The Free-Air Effect

Since the Earth's gravitational attraction is very nearly that of a sphere with central symmetry, it attracts as though its mass were concentrated at its centre. Thus, as one rises (increases) in elevation above sea level, the gravitational attraction will decrease as the inverse square of the distance to the centre of the Earth. Since possible elevation changes on the Earth are only on the order of 0.1% of the Earth's radius, we may determine the effect of a change ΔZ (m) in elevation in terms of the resultant change in gravity. This is termed the Free-Air effect, and is the mean vertical gradient of g , above the surface of the Earth. In fact, the actual Free-Air gravity gradient measured at the surface can vary by up to 25 percent from this theoretical value due to non-uniform density of the sub-surface rocks in the area.

3.2.8.2 The Bouguer Effect

When one increases elevation on the Earth, it usually implies that there is an additional mass between the original level and the new level. This additional mass itself will exert a positive gravitational attraction, which acts to reduce the Free-Air (negative) gravity change. The Bouguer gravity effect Δg_B is calculated on the basis of the gravitational attraction of a horizontal slab, of infinite extent and of thickness equal to the elevation difference.

3.2.8.3 The Elevation Effect

The Free-Air and Bouguer effects may be combined as the elevation effect. For gravimeter measurements made on the sea-bottom, the Bouguer effect is reduced by the difference between the density (d) of the underlying rock and that of the seawater (1.05 g/cm^3).

3.2.9 Terrain Effect

Local irregularities in the topography around a gravity station may give rise to significant effects. Hills rising above the station Fig. (3.2) will cause a reduction in gravity (upward pull) while valleys falling below the station Fig. (3.2) will also cause a reduction in gravity due to

the deficit of mass that would be included in the Bouguer assumption of an infinite slab. Thus, all topographic irregularities will cause a reduction in the observed gravity values.

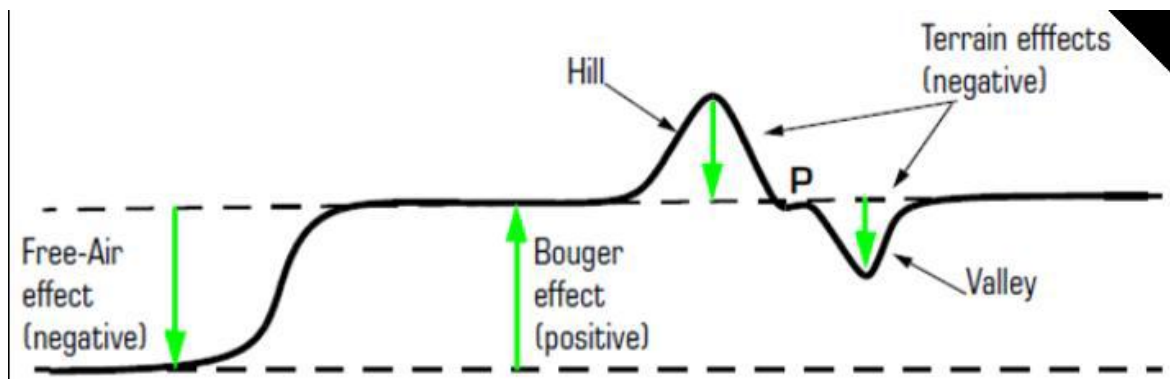


Fig 3.2 : Free Air, Bouguer and Terrain Effects.

3.2.10 Variation With Time

3.2.10.1 Earth Tides

The gravitational attraction of the Sun and the Moon are sufficiently large as to cause serious time-varying changes in the measured gravity values on the surface of the Earth, of as much as 0.3 mGal, in envelope. These tidal gravity effects may be calculated as a function of latitude, longitude of the station and the Universal Coordinated time (UTC) of the measurement, in accordance with various formulae.

Providing that the UTC time is entered to the nearest minute, the tidal gravity effects may be calculated to within a few μGal of their actual value at any location. There are however, residual tidal effects of this same order, due to tidal deformation of the Earth and the attraction of and loading effects of the oceans.

3.2.10.2 atmospheric Pressure

Changes in atmospheric pressure imply changes in the mass of the air column above the gravity point of measurement. An increase in atmospheric pressure will cause a decrease in the observed gravity, and vice-versa.

3.2.10.3 Ocean Tides (Sea Level Change)

Gravity measurements made near the sea coast may be directly affected by daily tidal changes, in the extreme, where a measurement is made on a cliff adjacent to deep water.

3.2.11 Variation With Geology

This is the very reason of gravity measurements. The various rock types and individual minerals which constitute the Earth each have their characteristic range of densities. The distribution in the subsurface of the constituent rock types and minerals will therefore, be reflected through changes in the local gravitational field. The variation, from place to place, of the gravitational field of the Earth may, therefore, be interpreted in terms of the subsurface geology with certain assumptions and limitations.

3.3 Satellite Gravity

The motion of a satellite orbiting the Earth is mainly caused by the gravitational field, together with non-conservative forces, like atmospheric drag and solar radiation pressure. In dynamic orbit determination, one makes use of a global gravity model, together with positioning techniques like GPS and satellite laser ranging (SLR). The inverse approach is to determine a global (homogeneously accurate) gravity model from orbit information of several satellites. This approach has been used since the launch of the first satellites, see, e.g., Buchar [1958], in which the oblateness of the Earth could be derived from an alternative data source, compared to the terrestrial and marine observations used so far. Satellite data has been the key data source for global gravity models, especially in recent years, with the launch of two dedicated gravity missions, the Challenging Mini-satellite Payload for Geophysical Research and Applications (CHAMP) mission and the GRACE mission, and with the upcoming Gravity Field and Steady-State Ocean Circulation Explorer (GOCE) mission, to be launched in September 2008.

These new satellite observations have already improved our knowledge about the static and time-varying gravity field of the Earth and have given new insights into the large scale processes in the interior of the Earth and the smaller (time-varying) changes on its (sub-) surface.

These satellites used radar altimeters to measure the height of the sea surface, from which free-air gravity was calculated.

4. DATA PROCESSING AND INTERPRETATION

4.1 Introduction

As mentioned earlier in chapter three, the used method in this study is gravity method that depends on densities variations. For the present work various data types, from different sources (ground and satellite gravity data) were made available. That individually constitute part of the spatial information system pertaining to the Melut area have been used. In the next sections the basic data characteristics, data processing and interpretation results will be provided. Geophysical data available to this work were obtained in the form of gravity point data for the ground gravity and regular grid of satellite gravity data.

4.2 Ground Gravity

These data were obtained through ground survey using gravimeter. The data have been corrected by all correction for gravity data as we mansion in Chapter Three. 1251 gravity points in the form of Bouguer Anomaly, distributed in the whole study area were gathered for the present study. The data were provided in table format containing three columns: longitude, latitude and the gravity values.

4.3 Satellite Gravity

The big advantage of satellite gravity data is that we can obtain a global coverage of the Earth. By tracking the orbit of a satellite, one can strengthen the estimation of the low-degree part of the gravitational field and fill in the gaps in some remote areas.

Altimetry is an accurate technique to obtain an estimate of the geoid in the oceanic regions. A constellation of multiple satellites, with an inter-satellite tracking, is able to obtain the temporal changes in the gravity field and gradiometer is used to estimate the high-degree spherical harmonics of the Earth's gravitational field.

It's another source of data, we received it in the form of FAA form (Free Air Anomaly) to three latitude lines (N8,N9,N10) reading range of longitude (20° 00'E -38° 00'E). So the data were filtered to the boundary of the study area with longitudes: 32° 00'E - 34° 00' E and latitudes: 8° 00'N - 10° 30' N.Together with the FAA data, the elevation for any point is delivered. After conducting the filtering process, the number of point becomes 18240 grid points. These data were corrected for BC (Bouguer correction) and consequently BA (Bouguer Anomaly) was computed using the following equations:

$$BC=0.04193*\rho*\text{elevation}$$

$\rho \equiv$ density (equal 2.67 g/cm³)

$$BA=FAA-BC$$

Accomplishing these calculations, the satellite data are completely prepared (Table 4.1), saved in excel sheet and ready for interpretation.

Table 4.1 : Sample of Ground data.

longitude	latitude	Bouguer Anomaly(BA)
32.4383	8.9944	-47.6
32.4439	8.9875	-48.2
32.3883	9.0997	-39.9
32.3917	9.0917	-40.2
32.3944	9.0825	-41
32.3972	9.0736	-41.3
32.4	9.0644	-41.5
32.4042	9.0558	-42.1
32.4083	9.0483	-42.8
32.4153	9.0436	-44.4
32.4222	9.0394	-45
32.4306	9.0333	-45.4
32.4361	9.0275	-45.5
32.4439	9.0208	-46
32.4403	9.0125	-46.7
32.4389	9.0031	-47
32.4417	9.0492	-43
32.4472	9.0547	-43.5
32.455	9.0606	-43.2
32.4611	9.0664	-42.5
32.4694	9.0719	-41.8

Table 4.2 : Sample of Satellite data and corrections.

long	lat	FAA	elev	BC	BA
32.0083	10.4992	-7.7	399	44.66929	-52.3693
32.025	10.4992	-9.1	397	44.44538	-53.5454
32.0417	10.4992	-10.6	397	44.44538	-55.0454
32.0583	10.4992	-12	397	44.44538	-56.4454
32.075	10.4992	-13.6	397	44.44538	-58.0454
32.0917	10.4992	-15.4	395	44.22147	-59.6215
32.1083	10.4992	-17.4	393	43.99757	-61.3976
32.125	10.4992	-19.7	393	43.99757	-63.6976
32.1417	10.4992	-22.1	393	43.99757	-66.0976
32.1583	10.4992	-24.7	395	44.22147	-68.9215
32.175	10.4992	-27.2	393	43.99757	-71.1976
32.1917	10.4992	-29.6	393	43.99757	-73.5976
32.2083	10.4992	-31.8	393	43.99757	-75.7976
32.225	10.4992	-33.7	393	43.99757	-77.6976
32.2417	10.4992	-35.3	393	43.99757	-79.2976
32.2583	10.4992	-36.7	391	43.77366	-80.4737
32.275	10.4992	-37.8	391	43.77366	-81.5737
32.2917	10.4992	-38.6	393	43.99757	-82.5976
32.3083	10.4992	-39.2	393	43.99757	-83.1976
32.325	10.4992	-39.4	393	43.99757	-83.3976
32.3417	10.4992	-39.4	393	43.99757	-83.3976
32.3583	10.4992	-39	393	43.99757	-82.9976
32.375	10.4992	-38.2	393	43.99757	-82.1976

4.4 Comparison Between Ground And Satellite Gravity Data:

Before starting processing and interpretation, there was an important question must be answered, what type of data (ground or satellite) is better to be used? To answer this question, a comparison between the ground and satellite gravity data was conducted. To this end, matching of ground gravity values with the corresponding values from the satellite gravity was performed. Using the SPOT function of the Spatial Analyst Tool of ArcGIS, the corresponding satellite gravity value to each ground gravity values was picked. These values were saved in tabular form for further statistical analysis and plotted in two curves as shown in Fig (4.1).

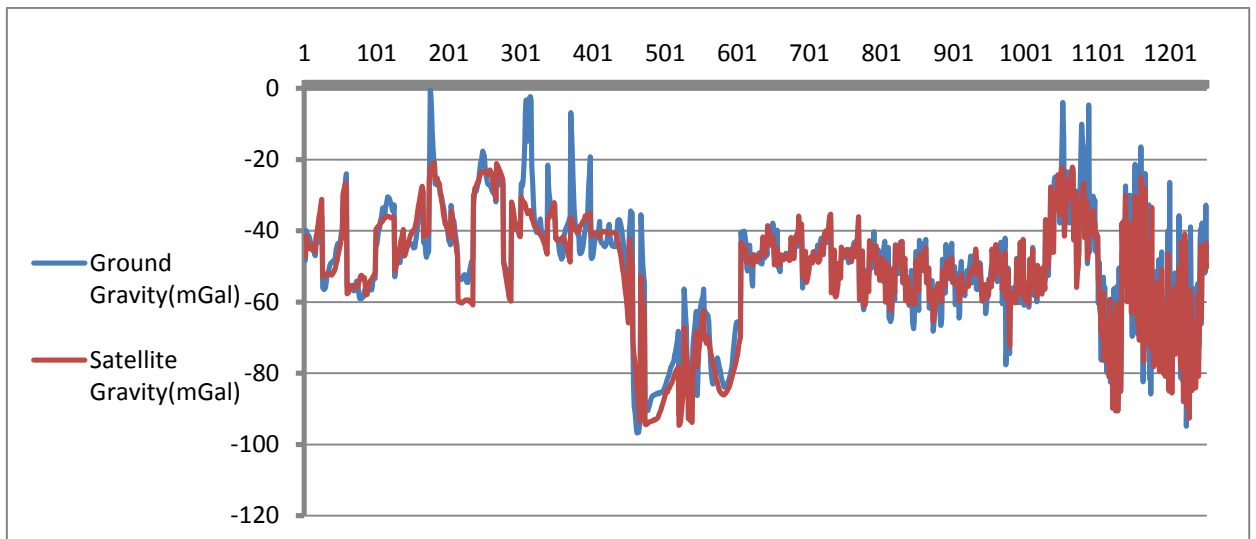


Fig 4.1 : Showing comparison between satellite and ground gravity.

From Fig (4.1), it is clear that the difference between the ground and satellite gravity data is very minor. Accordingly, satellite gravity data will be used in present study. This is because satellite gravity data are better than the ground measurement in many aspects including:

- Low cost.
- Good resolution (1.75 km).
- Good coverage.
- Easy to records.

4.5 Processing And Interpretation

4.5.1 Introduction

In this stage, processing of satellite data using many programs and interpretation of the results will be carried out. Firstly, satellite gravity data were imported into ArcGIS program, where gravity maps such as BA were prepared. Regional and residual maps with contour lines after separation between regional and residual, and interpret these maps to define the location of Basement and Sediment by the description of the resulting anomaly of gravity data. The explanation of the major features revealed by these data in terms of types of likely geological formations and structures were determined. Secondly, Oasis Montaj program was used to calculate the FVD (First Vertical Derivative), SVD (Second Vertical Derivative) and FHD (First Horizontal Derivative) of the gravity field. These Derivatives helped in fault detection and delineation after draw maps with suitable contour interval.

4.5.2 Bouguer Anomaly (Ba)

Before data processing, data was provided in Excel sheet form. This data were added to the ArcGIS, where a shape file for points was created. Interpolation of these points to a gravity surface was conducted using the Inverse Distance Weighted (IDW) algorithm. The gravity surface was then used to create contour lines with contour interval of 5mGal (Fig. 4.2).

From Figure (4.2), it is apparent that the Bouguer Anomaly values gradient from relatively high in the west and increase to very high values, and declined to lowest values in the center along the area from N to S. Increase to high values in eastern area is easily observable. The gradient in BA corresponds to the type of rocks in study area (Basement or Sediments). The maximum values of BA located in the western side and ranges between -35mGal - -25mGal that may reflect the basement rocks. On the other hand, the minimum values of BA are located in the center of the area and range between -70mGal - -90mGal corresponding to basinal area. The map also shows a number of faults as indicated by dense gradient belt of gravity anomaly and distortion zone of gravity anomaly contours and borderline of significant positive gravity anomaly and negative one. Faults defined in the region when BA was higher values and decline to lower values or opposite case.

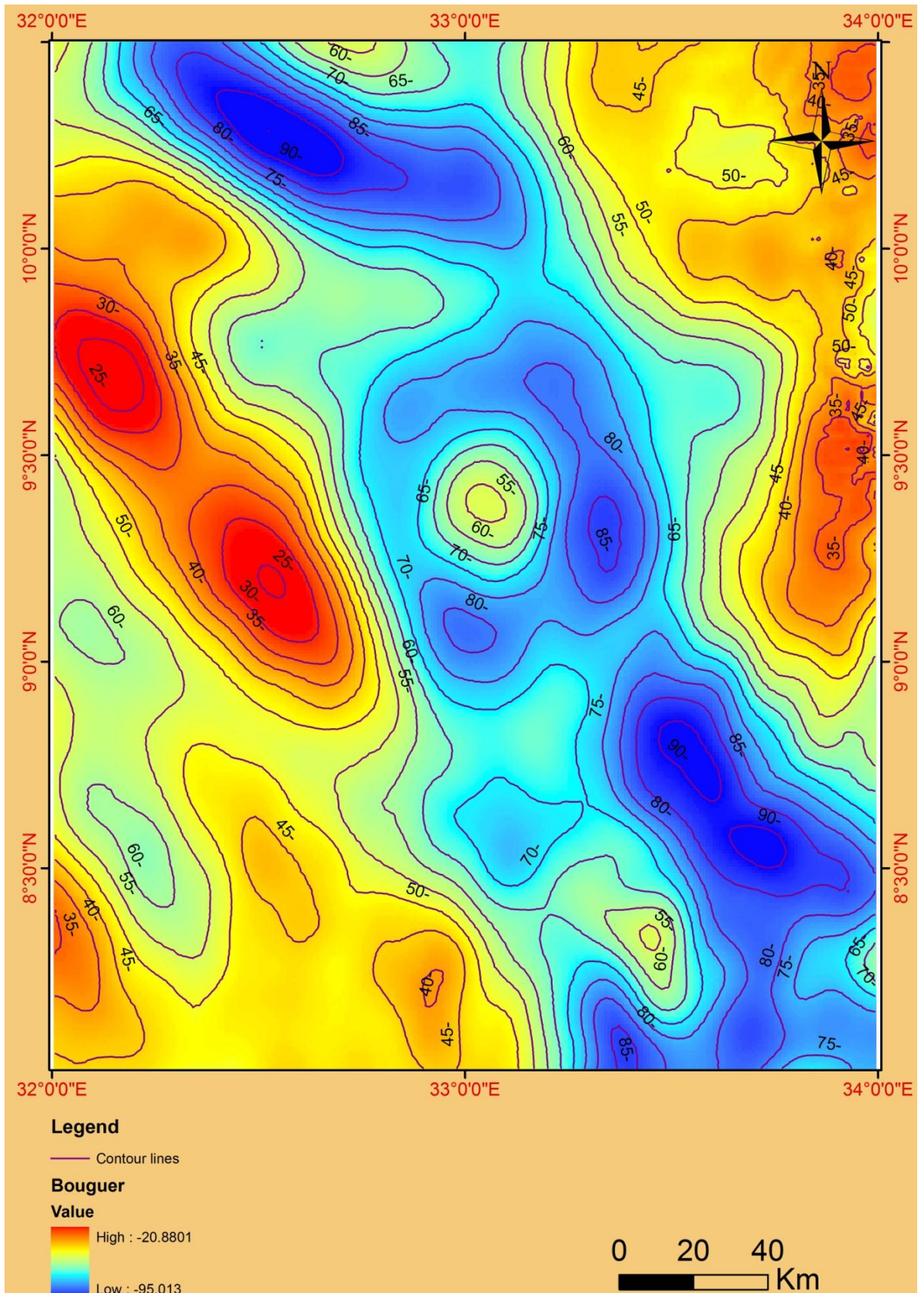


Fig 4.2 : Showing Bouguer Anomaly Gravity map for Melut region. Contour interval is 5mGal. Crosses lines are gravity model profiles.

4.5.3 Regional-Residual Anomaly Separation

Anomalies of interest are commonly superposed on a regional field caused by sources larger than the scale of study or too deep to be of interest. In this situation, it is important to perform a regional-residual separation, a crucial first step in data interpretation. Historically, this problem has been approached either by using a simple graphical approach (manually selecting data points to represent a smooth regional field) or by using various mathematical tools to obtain the regional field. Many of the historical methods are still in common use today.

The graphical approach initially was limited to analyzing profile data and, to a lesser extent, gridded data. The earliest non graphic approach used a regional field defined as the average of field values over a circle of a given radius, with the residual being the difference between the observed value at the center of the circle and this average.

Henderson (1960) showed that such averaging was equivalent to calculating the second vertical derivative except for a constant factor. He proposed using a least-squares fit to data to determine the regional field, an approach criticized, since the anomalies themselves will affect somewhat the determined regional. The effect of shallow sources could be removed through gravity modeling, proposed using 2D linear-wavelength filtering with filters of different cutoff wavelengths to solve the problem. The method was further expanded, who also used a cross correlation function to obtain trend directions from magnetic data.

Matched filter method can also be used for separating the residual field from the regional field. A method based on frequency-domain Wiener filtering was proposed by Pawlowski and Hansen (1990). Analyzed the shape of power spectra calculated from observed data. Clear breaks between low and high-frequency components of the spectrum were used to design either band-pass or matched filters.

Bouguer anomaly fields are often characterized by a broad, gently varying, regional anomaly on which may be superimposed shorter wavelength local anomalies. Usually in gravity surveying it is the local anomalies that are of prime interest and the first step in interpretation is the removal of the *regional field* to isolate the *residual anomalies*.

In the present study, Bouguer Anomaly map was created in a grid form using Fishnet Tool of Arc GIS, with cells size equal to 5*5 km², and pick the BA value in the center of any cell. The regional gravity component was calculated using the following equation:

$$\mathbf{Reg}_{ij} = \frac{\mathbf{Obs}(i,j+1) + \mathbf{Obs}(i+1,j) + \mathbf{Obs}(i-1,j) + \mathbf{Obs}(i,j-1)}{4*d}$$

Where:

i,j ≡ the number of row and column.

Obs ≡ observed gravity (mGal).

d ≡ distant between points (5km).

Reg ≡ regional gravity (mGal).

Accordingly, the residual anomaly was calculated using the following equation (Fig. 4.3):

$$\mathbf{Residual\ gravity} = \mathbf{Observed\ gravity} - \mathbf{Regional\ gravity}$$

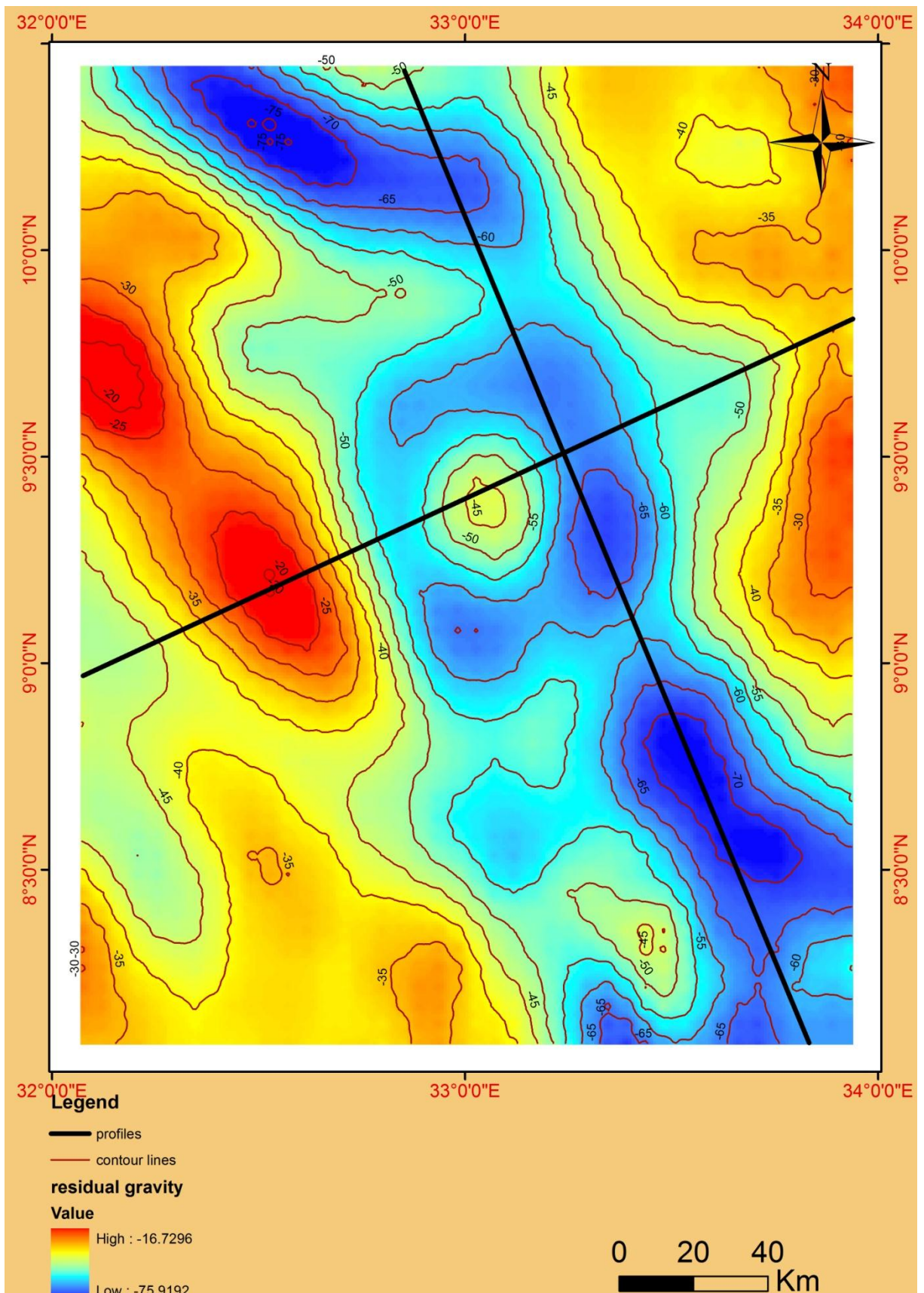


Fig 4.3 : The residual gravity map for study area. Contour interval is 5mGal. Black lines are the location of profiles used in gravity modeling.

4.5.4 Derivatives Of The Gravity Field:

From Bouguer anomaly (BA) records we use (Oasis Montaj) program to determine values of the First Vertical Derivative (FVD), Second Vertical Derivative (SVD) and First Horizontal Derivative (FHD) for some points in the study area. Then the data were exported as excel sheet and imported into the ArcGIS program to create a shape file for points. The data were then interpolated to a surface using an inverse distance weighted (IDW) techniques for (FVD, SVD and FHD). Finally, contour lines were generated with the suitable contour interval for each derivative.

4.5.4.1 First and Second Vertical Derivatives

The Second Vertical Derivative technique was used as two dimensional filters for interpretation of potential field data. The second derivative accentuates shallow anomalies and suppresses deep seated effects. Points of inflections of the second derivatives, i.e. points where the second derivative value changes its sign, are geologically expressed as faults, since the gravity gradient undergoes its most rapid changes from one level to another in the vicinity of faulted areas.

If we use the symbol (g) to represent the gravity and (z) is vertical downward axes, then the second derivative is the quantity d^2g/dz^2 . The importance of the second derivative for potential field interpretation arises from the fact that the double differentiation with respect to depth tends to emphasize the smaller, shallower geological anomalies at the expense of larger, regional feature.

The intent of applying the derivative technique in this study is to detect the surface and near surface faults. As shown in Figure (4.5), the derivative has a higher value at the greatest curvature (crest or trough) and has a zero value where there is no curvature i.e. at point of inflection; this phenomenon could geologically represented by the presence of a fault.

And first vertical derivative (FVD) has a similar effect to the second vertical derivative in emphasizing features related to gradients in the field rather than the field itself. It suffers less

from noise enhancement than the second vertical derivative and has an additional interesting use because it gives the gravity field gradient Fig(4.4).

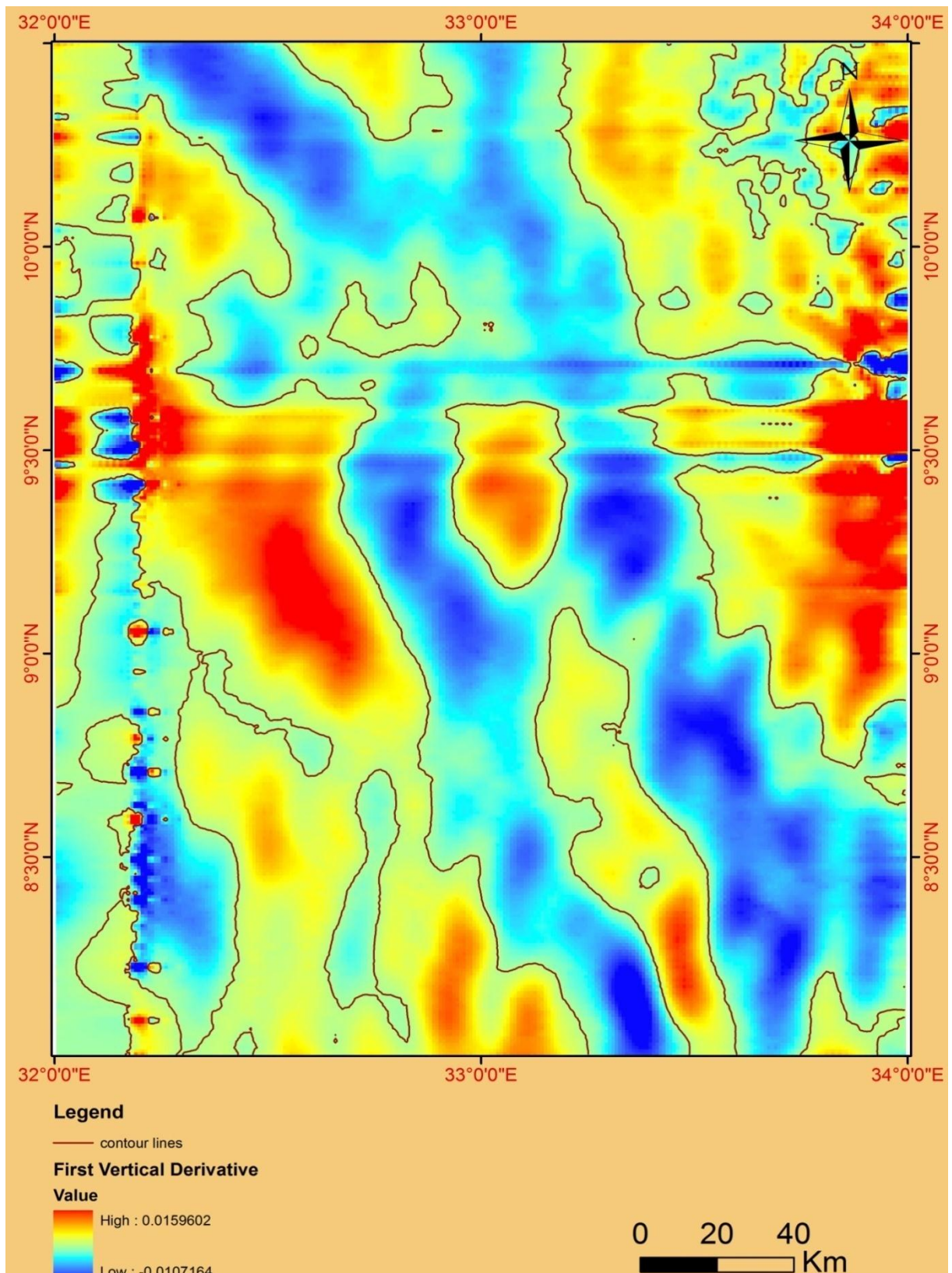


Fig 4.4 : First vertical derivative map and of the study area, on which the zero contours lines separates the positive from the negative anomalies.

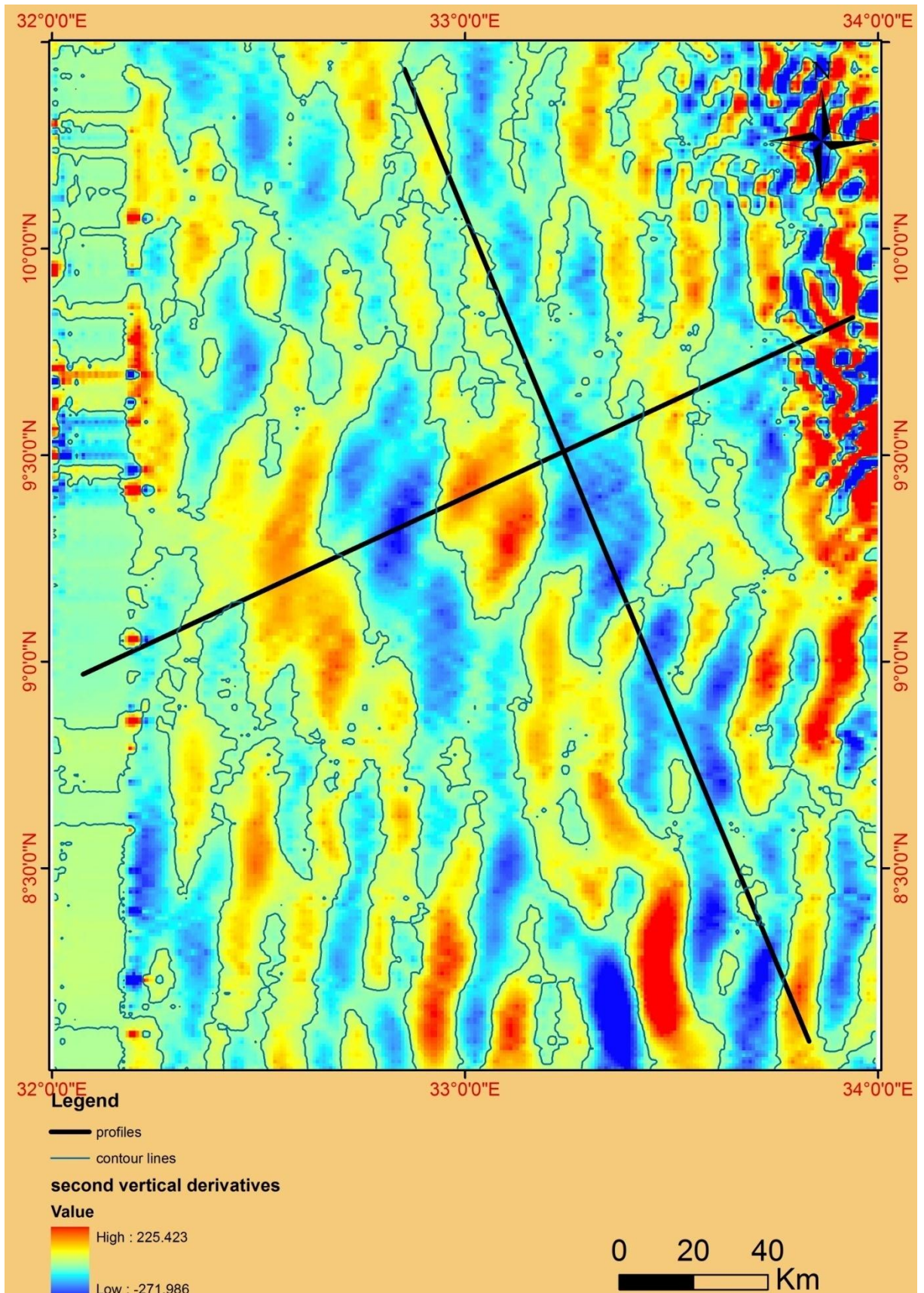


Fig 4.5 : The second vertical derivative map and of the study area, on which the zero contours line separates the positive from the negative anomalies.

4.5.4.2 First Horizontal Derivative

Can easily be computed in the space domain, are now the most common method for detecting target edges. The peaks in the magnitude of the total horizontal gradient of gravity data (square root of the sum of squares of the x - and y -derivatives) could be used to map near-vertical boundaries of contrasting densities, such as faults and geologic contacts.

The method became more widely used following subsequent papers discussing various aspects of the method and showing its utility. In map form, the magnitude of the horizontal gradient can be gridded to display maximum ridges situated approximately over the near-vertical lithological contacts and faults.

Figure (4.6) contains a linear maximum gradient trending E and W. The extension of maximum horizontal gradient zones and their orientation are utilized to determine faults extension and their orientations, respectively.

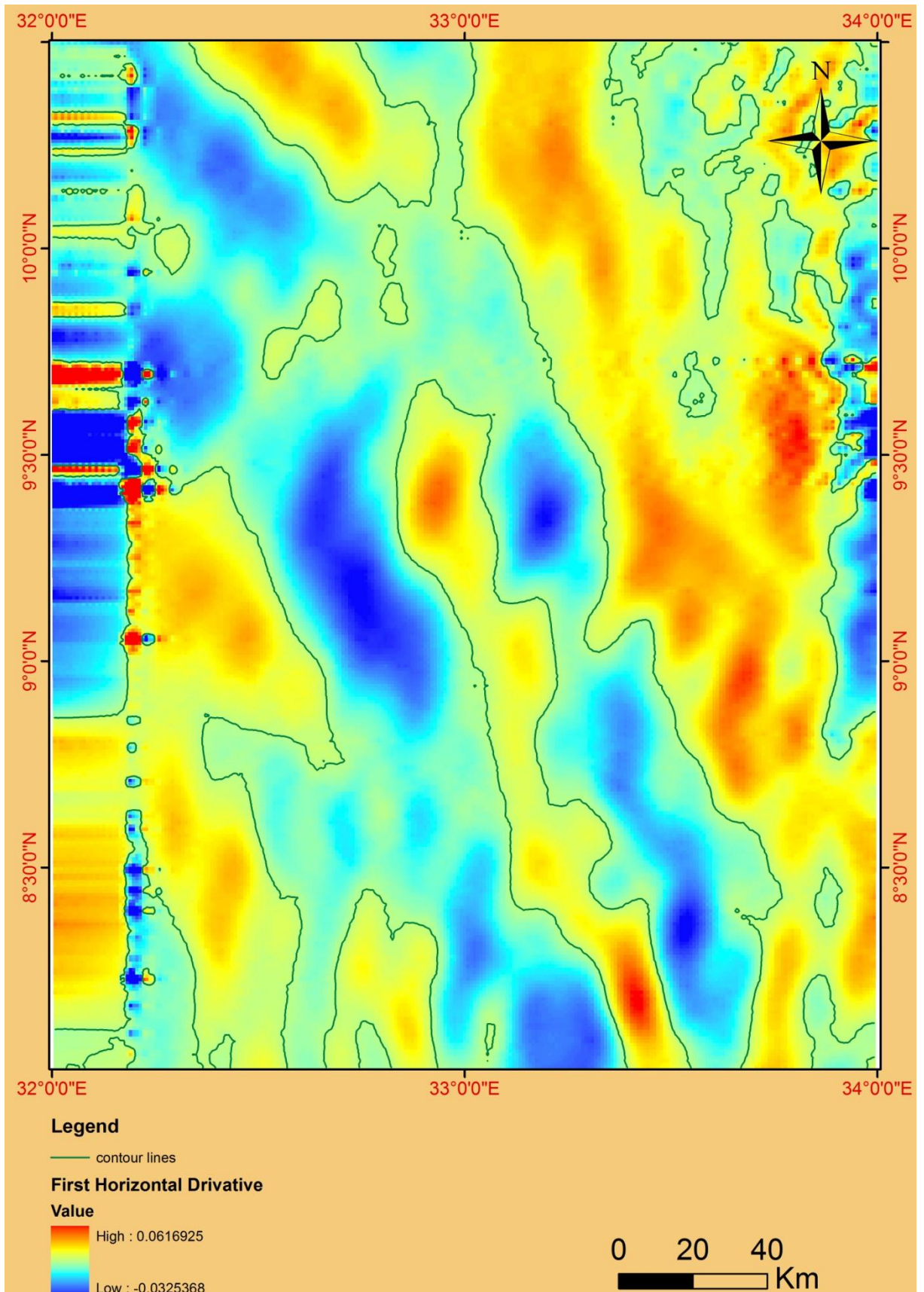


Fig 4.6 : First horizontal derivative map for Melut region, with zero contours line.

4.6 2.5D Gravity Modeling

The 2.5D modeling program (Gravmodel) was used to decipher the subsurface structure along two profiles in the study area. The program calculates the gravity anomaly due to the 2.5D bodies. It is based on the Talwani algorithm to calculate the gravity contribution of each body to the observed anomaly in an interactive way, so a change of a body does not require the recalculation of the whole model. The distances are measured in kilometers; the densities are in g/cm^3 and the anomalies in mGal.

The modeling consisted of fitting the observed anomalies and computed curves, based on bodies representing the possible geological units present in the subsurface. The density contrasts of rocks were calculated based on the difference between the mean density of the Earth's crust taken as 2.4 g/cm^3 and the various rock densities. The mean density of sedimentary formations has been taken 2.40 g/cm^3 in the study area. All profiles P1 and P2, which are directed SW-NE and NW-SE, are drawn from 47 and 61 points with separation of about 5 km (Fig. 4.7 and 4.9).

Model of Profile1

The profile contains 47 points from the residual anomaly map. The distance between points is kept equal to 5 km. This profile runs in the SW-NE direction (Fig. 4.7). The gravity along profile represent paired BA with relatively high values in the beginning and increase to very high and decline to low in the center. After that increase and decrease to lowest record along profile, and last increase at the end of profile. The thickness gradient along profile from shallow to deep, the maximum depth to the basement in the center is equal 4500m. There are many faults defined and indicated from Figure (4.8). All the geological structures are faults and all faults are normal fault caused due to the Central African Shear Zone (CASZ).

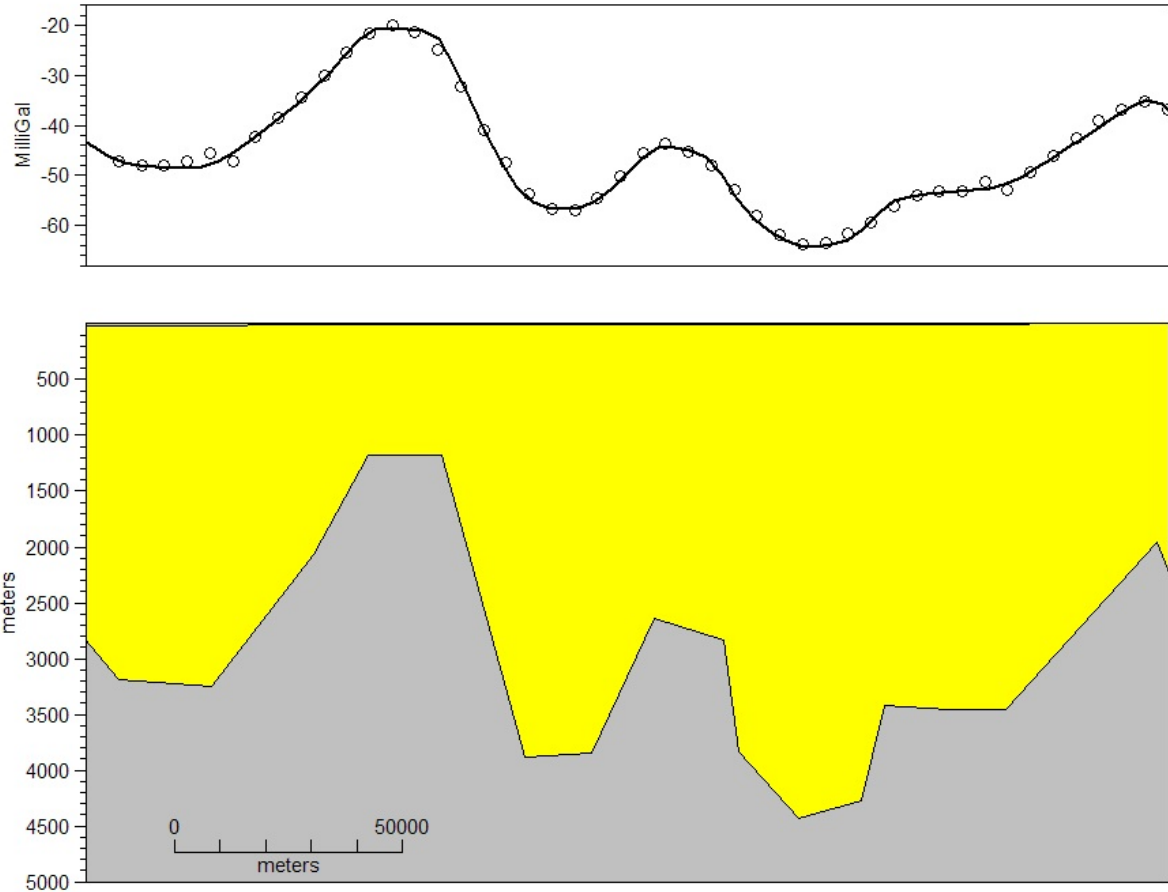


Fig 4.7 : Geological model of profile (1).

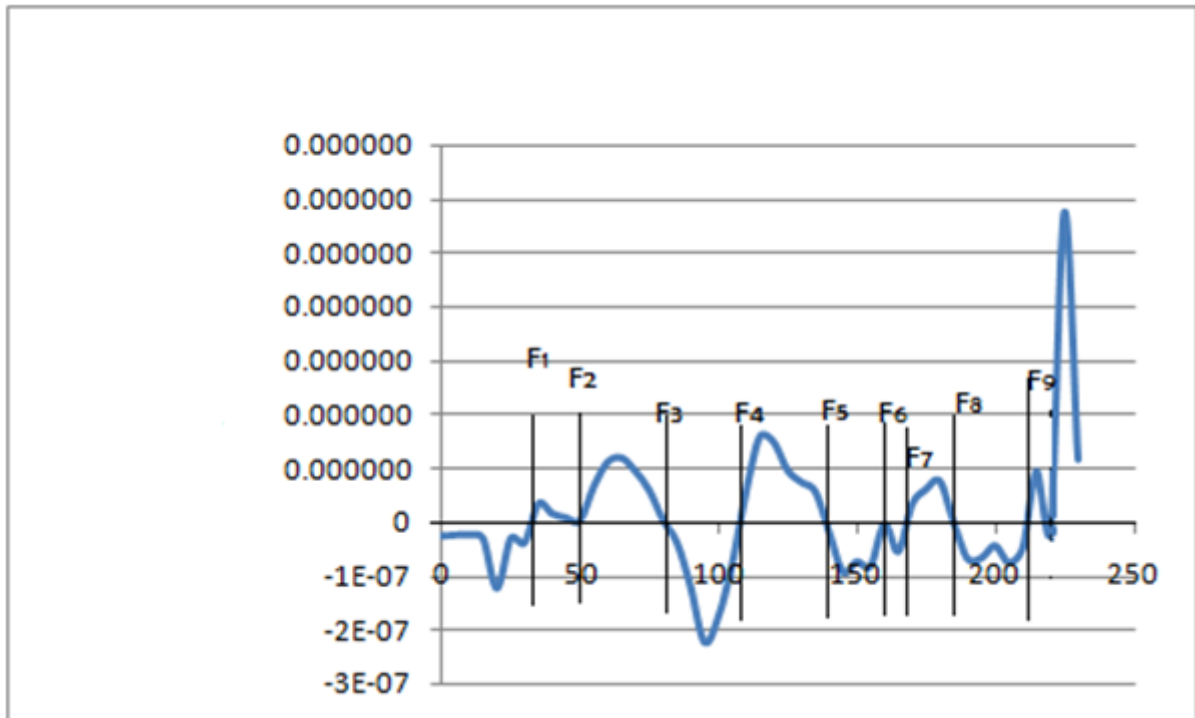


Fig 4.8 : Second vertical derivative (SVD) along profile 1. F stands for Fault.

Model of Profile2

The profile runs in the NW – SE direction and it passes across the center of sedimentary basin. This profile contains 61 points of BA from residual map. The distance between points is kept equal to 5km. We find different readings in this profile explained some geological structures. This difference in values is caused by the density contrasts. According to these differences, the basement and sedimentary rocks were delineated. There are many faults defined and indicated from Figure (4.10). The maximum depth to the basement in the center is equal 4800m.

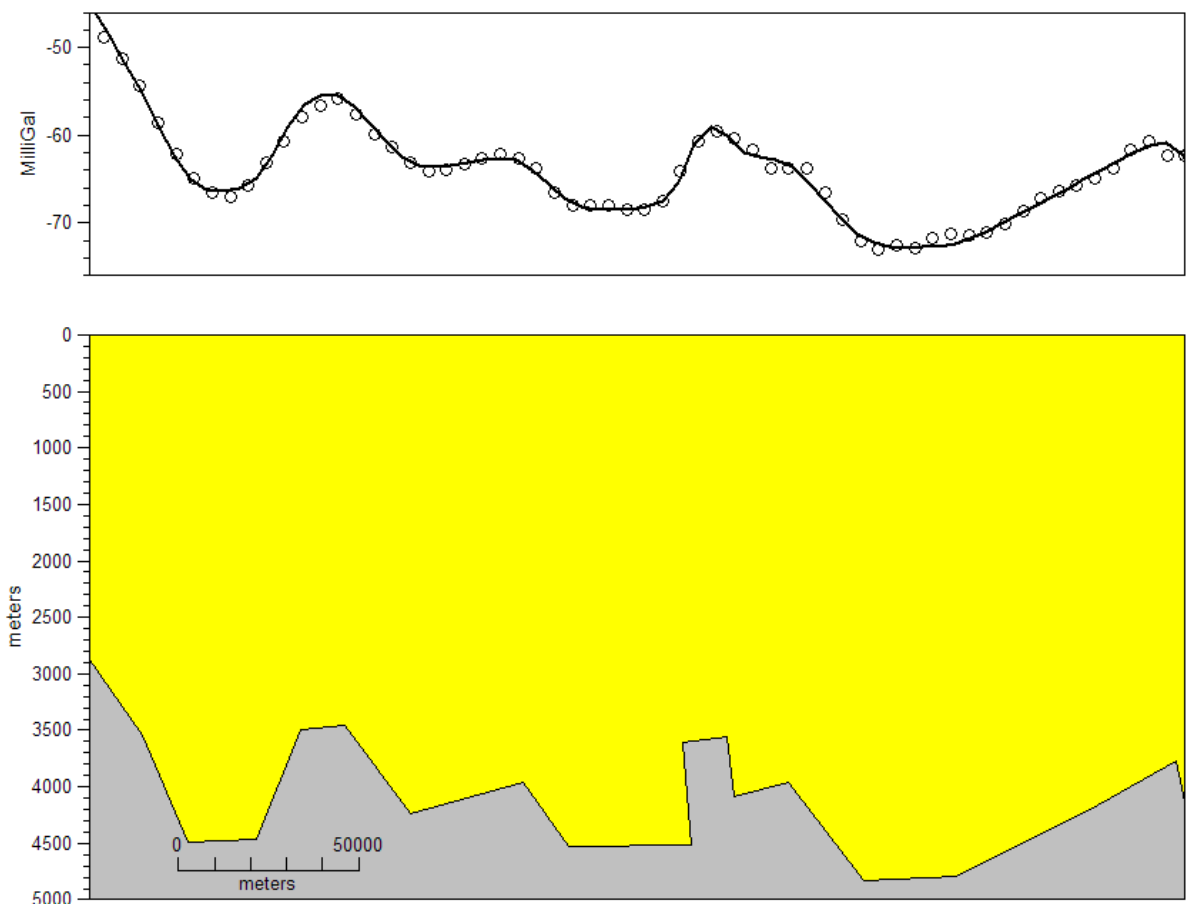


Fig 4.9 : Geological model of profile (2).

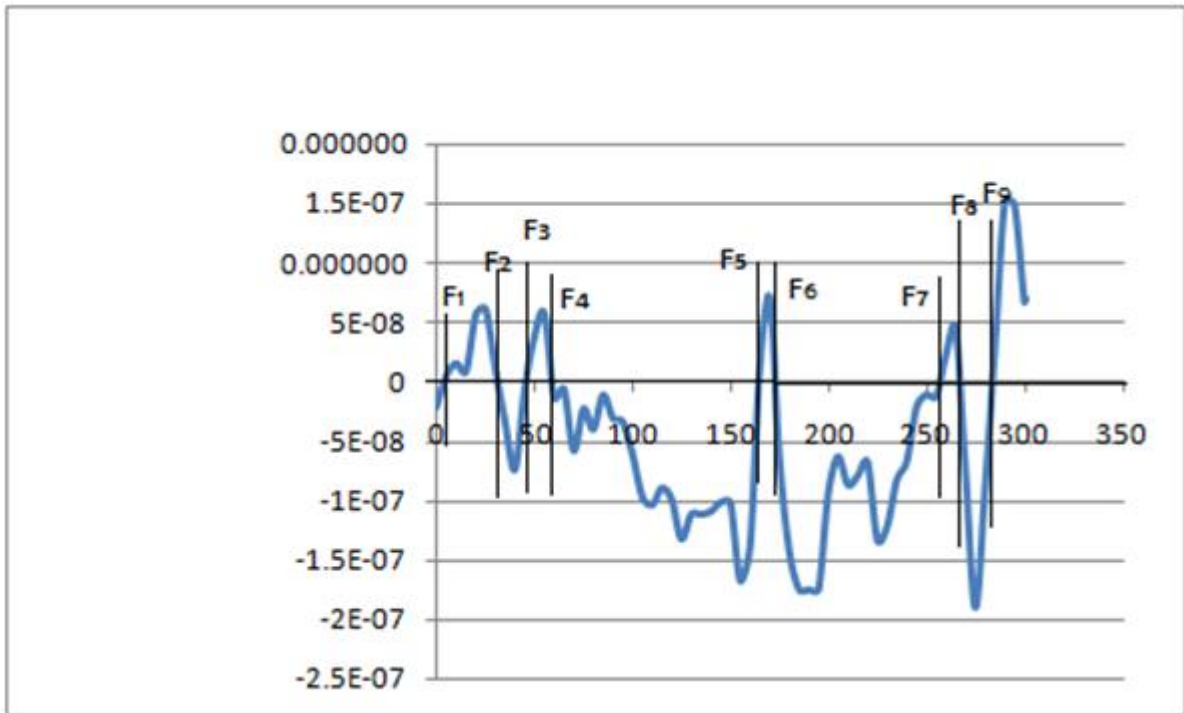


Fig 4.10 : Second vertical derivative (SVD) along profile 2. F stands for Fault.

5. CONCLUSION AND RECOMMENDATIONS

5.1 Conclusion:

The difference between the ground and satellite gravity data is very minor. Accordingly, satellite gravity data used in present study. This is because satellite gravity data are better than the ground measurement.

Average method was used in order to separate the regional from the residual component of the gravity. The Derivatives of the Gravity were computed in order to study the presence of faults. Moreover, two profiles were constructed across the residual gravity map in an approximately SW-NE and NW-SE directions cutting the most prominent anomalies in the area. 2.5D Gravity modeling established to decipher the subsurface structure along two profiles in the study area.

The results of interpretation maps and profiles defined boundary of Basin, identified there was many Faults in the study area and computed depth of Basement along profiles.

5.2 Recommendations:

Gravity survey make good information about major structures but it is not in minor, So in future or next study there are some remarks we suggest it :

- Using with Gravity survey other methods to give more accuracy.
- Study drilled wells to provide more depth information.
- More focus of the southern part of melut Basin.

References

- Abdel Salam, M. G. & Dawoud, A. S. (1991):** The Kabus Ophiolitic Mélange, Sudan, And Its Bearing On The Western Boundary Of The Nubian Shield.- *Journal Of The Geological Society, London.*
- Andrew, G. (1948):** The Geology Of The Sudan.- In J. D. Tothill (Eds.), Agriculture In The Sudan, *Oxford University Press.*
- Awad, M. Z. (1994):** Stratigraphic, Palynological And Palaeoecological Studies In The East-Central Sudan (Khartoum And Kosti Basins), Late Jurassic To Mid-Tertiary.- *Berliner Geowiss. Abh. A.*
- Bosworth, W. (1992):** Mesozoic And Early Tertiary Rift Tectonics In East Africa.- In: C. J. Ebinger, H. K. Gubta & I. O. Nyambok (Eds.), Seismology And Related Sciences In Africa.- Tectonophysics.
- Buchar, E. (1958). *Motion of the nodal line of the second Russian Earth satellite (1957 β) and flattening of the Earth*, Nature.
- Cooper, G.R.J., (2003):** Grav2dc. 2.10. An Interactive Gravity Modeling Program For Microsoft 2050, South Africa Windows. School Of Geosciences, University Of The Witwatersrand, Johannesburg
- Dobrin, M. (1976):** Introduction To Geophysical Prospecting. New York Mcgraw-Hill, Book Company.
- Eisawi (2007):** Palynological And Palaeoenvironmental Interpretation Of The Late Cretaceous To Tertiary Strata Of The Melut Basin (Southeast Sudan)
- El Ageed, A. I. & El Rabaa, S. M. (1981):** The Geology And Structural Evolution Of The Northeastern Nuba Mountains, Southern Kordofan Province, Sudan.- *Bull. Geological Mineral Resources, Sudan.*
- El Shaafie, A. A. (1975):** Lithology Of The Umm Ruwaba Formation And Its Paleogeography In Connection With Water Problems.- Ph. D. Thesis, Institute Of Geol. Res., Moscow.
- Getaneh, A. (1981):** Gohatsion Formation. A New Lias-Malm Lithostratigraphic Unit From The Abayriver Basin, Ethiopia.– Geosci.
- Henderson, R.G. And Zietz, I. (1949):** The Computation Of Second Vertical Derivatives Of Geo Magnetic Field. Geophysics.
- Jasper Van Loon.(2008):** Functional And Stochastic Modelling Of Satellite Gravity Data.
- Kaska, H. V. (1989):** A Spore And Pollen Zonation Of Early Cretaceous To Tertiary Non-Marine Sediments Of Central Sudan.- *Palynology.*

Kazmin, V. (1973): Geological Map Of Ethiopia.- Addis Ababa, Geological. Survey, Ethiopia.

Khalid A. Elsayed Zeinelabdein1,* , Mohammed S. Elemam1, Hamdi A. Ali2, Osman M. Alhassan (2014): An Integrated Analysis Of Landsat Oli Image And Satellite Gravity Data For Geological Mapping In North Kordofan State, Sudan.

Klitzsch And Lejal-Nicol, (1984) Klitzsch, E. & Lejal- Nicol, A. (1984): Flora And Fauna From Strata In Southern Egypt And Northern Sudan.- Berliner Geowiss. Abh.

Mohammed. S.A. El Emam,(2012): Interpretation Of Gravity And Remote Sensing Data For Improved Geological Mapping North Of Port Sudan Area - Red Sea Region – Sudan.

Morelli,C., Gantor,C., Honkasalo,T. Et Al. (1971): The International Gravity Standardisation Net. Pub. Spec. No. 4 Du Bulletin Géodésique.

ROBERTSON RESEARCH INTERNATIONAL (RRI) & THE GEOLOGICAL RESEARCH AUTHORITY OF SUDAN (GRAS) (1991): The geology and petroleum potential of southern, central and eastern Sudan.

Nettleton, L.L. (1976): Gravity And Magnetics In Oil Exploration. Mcgraw-Hill, New York.

Sabins. F.F. (2000): Remote Sensing, Principles And Interpretation, 3rd Edition.

Sakuma, A. (1986): Second Internal Comparison Of Gravimeters. Internal Report, Bureau International Des Poids Et Mesures.

Schull, T. J. (1988): Rift Basins Of Interior Sudan: Petroleum Exploration And Discovery.- American Association Of Petroleum Geologists, Bull.

Vail, (1988): Lexicon Of The Geological Terms For The Sudan, 199 Pp.- Rotterdam/ Brookfield, (A. A.Balkema).

Vail, J. R. (1978): Outline Of The Geology And Mineral Deposits Of The Democratic Republic Of Sudan And Adjacent Areas.- Overseas Geological And Mineral Resources, London.

Whitcomb, J.H. (1987): Surface Measurements Of The Earth's Gravity Field. In: Samis, C.G. & Henyey, T.L. (Eds), Methods Of Experimental Physics, Vol. 24, Part B – Field Measurements. Academic Press, Orlando.

Whiteman, A. J., (1971): The Geology Of The Sudan Republic. Clarendon Press, Oxford.

[Http://Www.Petrodar.Com/Partners.Html](http://Www.Petrodar.Com/Partners.Html)